

Supplemental Figure Legends

Figure S1. Long-term ID inactivates mTORC1

(A) Levels of non-heme iron in response to 150 μ M DFO for 24 hours in HEK293T cells (n=5 replicates, unpaired t-test, mean \pm SE). (B) mRNA levels of *TTP* and *TFRC* at various time points after addition of 150 μ M DFO in HEK293T cells. Internal control: *POLR2A* (n=6 replicates per condition, one-way ANOVA and Tukey's post-hoc test, mean \pm SE). (C) Immunoblot of mTORC1 activity 18 hours after treatment with indicated concentrations of DFO ranging from 0 to 150 μ M in HEK293T cells. (D) Immunoblot of mTORC1 activity in response to 3 hours of with 150 μ M DFO or 50 μ M BPD in HEK293T cells. (E) mRNA levels of *TFRC*, *REDD1*, and *TTP* 3 hours after addition of 150 μ M DFO or 50 μ M BPD. Internal control: *POLR2A* (n=4-8 replicates per condition, one-way ANOVA and Tukey's post-hoc test, mean \pm SE). (F) Immunoblot of mTORC1 activity in response to 250nM Torin1 at indicated time points.

Figure S2. Iron chelation inhibits mTORC1 activity independent of cell cycle.

(A) Immunoblot of *TFRC* and mTORC1 activity in freshly isolated primary murine hepatocytes 18 hours after treatment with increasing concentrations of DFO. (B) mRNA of *Ttp* and *Tfrc* in primary murine hepatocytes in response to indicated concentrations of DFO for 18 hours. Internal control: *Polr2a* (n=3 replicates per condition, one-way ANOVA and Tukey's post-hoc test, mean \pm SE). (C) Immunoblot of mTORC1 activity in hPS-CM 18 hours after treatment with 150 μ M DFO. (D) Immunoblot of mTORC1 activity in hiPS-neurons 18 hours after treatment with 150 μ M DFO. (E) Immunoblot of HEK293T cells chelated for 18 hours with 150 μ M DFO followed by the readdition of 300 μ M ferric ammonium citrate (FAC) for indicated times.

Figure S3. Iron chelation inhibits cell cycle but does not cause cell death within 24 hours.

(A) Fluorescent microscopy of BrdU incorporation in HEK293T cells treated with 150 μ M DFO for 12 hours. (B) Quantification of cellular proliferation by Hoescht staining of nuclei 48 hours after treatment with DFO (n=6 replicates, unpaired t-test, mean \pm SE). (C) Fluorescent microscopy of cell death using Hoescht and propidium iodide (PI) double staining in HEK293T cells treated with 150 μ M DFO for 0-24 hours or 250nM Torin-1 for 24 hours. (D) Quantification of images in panel C. (n=6 replicates, one-way ANOVA and Tukey's post-hoc test, mean \pm SE).

Figure S4. Reducing Transferrin saturation in the culture media and overexpressing the iron exporter Ferroportin inhibits mTORC1 activity.

(A) Immunoblot of mTORC1 activity in HEK293T cells treated with high Tf-sat (66%) or low Tf-sat (6.6%) media for 18 hours. (B) Summary of immunoblot in panel A (n=3 replicates, unpaired t-test, mean \pm SE). (C) Immunoblot of mTORC1 activity in HepG2 cells transfected with the FPN-GFP fusion protein and TET inducible rtTA3 plasmids in the presence and absence of 500ng/ml doxycycline for 48 hours. (D) Summary of immunoblot in panel C (n=3 replicates, unpaired t-test, mean \pm SE). (E) Fluorescent microscopy of cells transfected with FPN-GFP construct and treated with 500ng/ml doxycycline for 24 hours demonstrating appropriate expression and localization of the FPN-GFP fusion protein. (F) Immunoblot of puromycin incorporation in rtTA3/FPN-GFP stable HEK293T cells in the presence and absence of 500ng/ml doxycycline for 48 hours. (G) mRNA expression of ER stress makers *CHOP* and *BNIP3* in HepG2 cells transfected with rtTA3/FPN-GFP plasmids and treated with 500ng/ml doxycycline for 48 hours. Internal control: *18S* (n=4 replicates, unpaired t-test, mean \pm SE).

Figure S5. Analysis of mTORC1 core complex expression and mitogen signaling pathways and mitochondrial function during ID.

(A) Immunoblot of protein levels of the key components of the mTORC1 complex after 24 hours of 150 μ M DFO in HEK293T cells. (B) Summary of results shown in panel A (n=4 replicates, unpaired t-test, mean \pm SE). (C) Immunoblot of total and phosphorylated TSC2, AKT, ERK, GSK3 β , and S6 proteins and total P53 at different time points after treatment with 150 μ M of DFO in HEK293T cells. (D) Immunoblot of mTORC1 activity and mitochondrial function in HepG2 cells treated with DFO for 18 hours at the indicated doses. (E) Oxygen Consumption Rate (OCR) measured by the Seahorse Assay in HepG2 cells treated for 24 hours of DFO at the indicated doses (n=8-10 replicates per group).

Figure S6. TSC2 complex and REDD1 are not required for mTORC1 inhibition during ID, and ID activates AMPK signaling.

(A) *Ttp* mRNA in WT and *Tsc2* KO MEFs in the presence and absence of 150 μ M DFO for 18 hours. Internal control: *Snrk* (n=4 replicates per condition, one-way ANOVA and Tukey's post-hoc test, mean \pm SE). (B) Immunoblot of mTORC1 activity in WT and *Tsc2* KO MEFs that were serum starved overnight followed by the addition of serum for 1 hour in the presence or absence of 150 μ M DFO for 17 hours (C) *REDD1* mRNA in HEK293T cells in response to *REDD1* siRNA. Internal control: *POL2RA* (n=6 replicates per condition, unpaired t-test, mean \pm SE). (D) *TFRC* mRNA in HEK293T cells in response to *REDD1* siRNA and 150 μ M DFO for 18 hours. Internal control: *POL2RA* (n=6 replicates per condition, one-way ANOVA and Tukey's post-hoc test, mean \pm SE). (E) Immunoblot of mTORC1 and AMPK activity in the presence of DFO or serum starvation with AICAR (an AMPK activator). (F) *Ttp* mRNA in the presence and absence of 150 μ M DFO for 18 hours in WT and *Ampka1/2* dKO cells. Internal control: *Polr2a* (n=4 replicates per condition, one-way ANOVA and Tukey's post-hoc test, mean \pm SE).

Figure S7. Iron chelation inhibits mTORC1 activity independent of alterations in mitochondrial metabolism.

(A) Targeted metabolomics in HEK293T cells treated with 150 μ M DFO for 18 hours (n=4 replicates per condition, Mann-Whitney test, median \pm quartiles). (B) Total cellular ATP pools in HEK293T cells after 18 hours of treatment with 150 μ M DFO (n=4 replicates per condition, Mann-Whitney test, median \pm quartiles). (C) Immunoblot of mTORC1 activity in HEK293T cells in the presence and absence of 150 μ M DFO for 18 hours, supplemented with 1mM dimethyl malate or 500 μ M NMN. (D) Immunoblot of mTORC1 activity in HEK293T cells in the presence and absence of 150 μ M DFO for 18 hours, supplemented with 100 μ M nucleoside cocktail (Adenosine, Guanosine, Thymidine and Cytidine), or 500 μ M dimethyl aspartate.

Figure S8. ID does not impair lysosomal acidification, and Leucine insensitive mTORC1 cell lines are resistant to inhibition by ID but have increased cell death.

(A) Fluorescent confocal microscopy image of acridine orange staining in HEK293T cells treated with 150 μ M DFO for 24 hours. (B) Summary of the results in Panel A (n=6-7 replicates per condition, unpaired t-test, mean \pm SE). (C) Total leucine levels in HEK293T cells treated with 150 μ M DFO for 24 hours (n=4-5 replicates per condition, Mann-Whitney test, median \pm quartiles). (D) SAM levels in HEK293T cells treated with 150 μ M DFO for 18 hours measured by HPLC-MS (n=4-5 replicates per condition, Mann-Whitney test, median \pm quartiles). (E) Immunoblot of mTORC1 activity in WT and *NPRL2* KO HEK293T cells deprived of leucine for 16 hours and restimulated with 400 μ M leucine for 1 hour. (F) Fluorescent microscopy of cell death using Hoescht and propidium iodide (PI) double staining in WT and *NPRL2* KO HEK293T cells treated with 150 μ M DFO for 0, 36 and 60 hours. (G) Quantification of images in panel F. (n=6 replicates, one-way ANOVA and Tukey's post-hoc test, mean \pm SE). (H) Immunoblot of mTORC1 activity in *Rraga*^{+/+} (WT) and *Rraga*^{Q66L/Q66L} (KI) MEFs treated with 150 μ M DFO for 18 hours. (I) Densitometry analysis of immunoblot in panel H. (n=3 replicates per condition, one-way ANOVA and Tukey's post-hoc test, mean \pm SE).

Figure S9. ID suppresses leucine uptake and leucine transporter expression and cell-permeable leucine re-localizes mTORC1 to the lysosome during ID

(A) ^3H -leucine uptake into MEFs treated with 150 μM DFO for 24 hours (n=5-6 replicates per condition, unpaired t-test, mean \pm SE). (B) ^3H -Leucine-leucine uptake into MEF cells treated with 50nM rapamycin for 24 hours (n=5-6 replicates per condition, unpaired t-test, mean \pm SE). (C) ^{14}C -Leucine uptake into HEK293T cells transfected with rtTA3/FPN-GFP or rtTA3/eGFP control and in the presence and absence of 500ng/ml doxycycline treatment for 48 hours or 150 μM of DFO for 18 hours (n=5-6 replicates per condition, one-way ANOVA and Tukey's post-hoc test, mean \pm SE). (D) mRNA of various leucine transporters in HepG2 cells transfected with rtTA3/FPN-GFP plasmids in and treated with 500ng/ml doxycycline for 48 hours. Internal control: *18S* (n=5-6 replicates per condition, unpaired t-test, mean \pm SE). (E) *Slc38a9* mRNA levels in MEFs treated with DFO for 24 hours. Internal control: *Polr2a* (n=8 replicates per condition, unpaired t-test, mean \pm SE). (F) *TFRC* mRNA levels in HeLa cells treated with 150 μM DFO for the indicated time points. Samples matched with Figure 4D. Internal control: *POLR2A* (n=4 replicates per condition, one-way ANOVA and Tukey's post-hoc test, mean \pm SE). (G) Immunoblot of mTORC1 activity in cytosolic fraction and LAT3 and PAT1 in the membrane fraction of HeLa cells treated with 150 μM DFO for 18 hours. (HA) Normalized expression (NX) of *SLC43A1* across multiple human tissues (<https://www.proteinatlas.org/ENSG00000149150-SLC43A1/tissue>). (I) Table listing the normalized expression of leucine transporters in the liver. Data for panels A and B was acquired from The Human Protein Atlas version 20.1 and Ensembl version 92.38, available from <http://www.proteinatlas.org> "Uhlén M et al., **Tissue-based map of the human proteome.** *Science* (2015) PubMed: [25613900](https://pubmed.ncbi.nlm.nih.gov/25613900/) DOI: [10.1126/science.1260419](https://doi.org/10.1126/science.1260419)". (J) Recruitment of mTORC1 to the lysosome in HEK293T cells treated with 150 μM DFO for 18 hours and supplemented with 400 μM LLMOE for 1 hour. (K) Summary of the results in panel A (n=6 replicates per condition, one-way ANOVA and Tukey's post-hoc test, mean \pm SE).

Figure S10. ID causes global hyper-methylation of histones

(A-B) Unbiased measure of global changes in histone methylation measured by histone-MS in response to ID. Graphs are presented as rank ordered lists by change in %abundance with 150 μM DFO - control (A) and total %abundance in the 150 μM DFO group (B). Data matched with Figure 5B.

Figure S11. ID and decreased transferrin saturation increase H3K9 di-methylation independent of cell-cycle, and ID represses mTORC1 activity and increases H3K9 di-methylation independent of ARNT, ATF4, and IRP system.

(A) Immunoblot of H3K9me² in hiPS-CM 18 hours after treatment with 150 μM DFO. Data paired with Figure S2C (B) Immunoblot of H3K9me² in hiPS-Neurons 18 hours after treatment with 150 μM DFO. Data paired with Figure S2D (C) Immunoblot of mTORC1 activity and H3K9me² levels in MEFs treated with high Tf-sat (66%), low Tf-sat (6.6%), or high Tf-sat (66%) media supplemented with 150 μM DFO for 24 hours. (D, E) Summary of immunoblot in panel C (n=3 replicates, one-way ANOVA and Tukey's post-hoc test, mean \pm SE). (F) Immunoblot of H3K9me² in HepG2 cells transfected with rtTA3/GFP-FPN plasmids and treated with 500ng/ml doxycycline for 48 hours. Data paired with Figure S4C (G) mRNA of *Ttp* and *Redd1* in WT and *Arnt* KO MEFs treated with 150 μM DFO for 12 hours. Internal control: *18S* (n=4 replicates per condition, one-way ANOVA and Tukey's post-hoc test, mean \pm SE). (H) Immunoblot of mTORC1 activity and H3K9me² levels in WT and *Atf4* KO MEFs treated with 150 μM DFO for 18 hours. (I) Summary of immunoblot in panel H (n=3 replicates per condition, one-way ANOVA and Tukey's post-hoc test, mean \pm SE). (J) Immunoblot of the IRP targets FPN and FTH1, and

H3K9me² levels in WT and *Irp1/2* KD/KO MEFs treated with 150μM DFO for 18 hours. **(K)** Summary of immunoblot in panel J (n=3 replicates per condition, one-way ANOVA and Tukey's post-hoc test, mean ± SE). **(L)** Immunoblot of the IRP1 levels in *Irp2* KO MEFs treated with control or siRNA targeted against *Irp1*. **(M)** Summary of immunoblot in panel L (n=3 replicates per condition, unpaired t-test, mean ± SE). **(N)** mRNA of *Irp1*, *Tfr1*, *Ttp* and *Lat3* in WT and *Irp1/2* KD/KO MEFs treated with 150μM DFO for 18 hours. Internal control: *Snrk* (n=6 replicates per condition, one-way ANOVA and Tukey's post-hoc test, mean ± SE).

Figure S12. Increased H3K9 di-methylation during iD is upstream of mTORC1 and cannot be rescued by supra-physiologic levels of α-KG or cell-permeable leucine.

(A) Ratio of 2-HG/succinate levels in HEK293T cells treated 150μM DFO for 18 hours measured by HPLC-MS (n=4-5 replicates per condition, Mann-Whitney test, median ± SE). **(B)** Immunoblot of mTORC1 activity and H3K9me² in HEK293T cells treated with 150μM DFO in the presence and absence of 1mM cell permeable dimethyl α-KG (DMKG). **(C)** Immunoblot of mTORC1 activity and H3K9me² in HEK293T cells starved of leucine for 16 hours in the presence or absence of 150μM DFO followed by supplementation with 400μM LLOME for 1 hour.

Figure S13. ID alters occupancy of POLR2A at the promoters of multiple genes.

(A) Fold change in POLR2A occupancy within predefined regions of the promoter and gene body to categorize genes defined by increased POLR2A binding, POLR2A loss, and promoter-pausing. **(B)** Gene-ontology (GO) terms of genes enriched in the increased POLR2A group after ID. **(C)** GO terms of genes that had lost POLR2A after ID. **(D)** UCSC genome browser tracks for the *LAT3* (top) and *PAT1* (bottom) gene loci. POLR2A and H3K9me² tracks from ChIP-seq analysis were loaded and represented as the difference in normalized reads between the DFO and control groups. Regions of H3K9me² enrichment in the DFO group are underlined in red. Direction of transcription is indicated by a black arrow. Encode Histone (*LAT3* and *PAT1*) and Genehancer (*PAT1*) browser tracks are displayed beneath and represent predicted enhancer regions which align with regions of increased H3K9me² signal in response to DFO. Yellow bar, red and grey arrows indicate enhancer regions designated by Encode Histone and Genehancer browser tracks.

Figure S14. ID increases H3K9 di-methylation within the promoter of *RPTOR* and correlates with decreased *RPTOR* mRNA expression.

(A) H3K9me² signal and POL2RA occupancy in the promoter for *RPTOR* from ChIP-Seq analysis. **(B)** ChIP-PCR of *RPTOR* in HEK293T cells. Cells treated with 150μM DFO or 250μM IOX1 for 12 hours and vehicle controls were followed by IP of lysates using an antibody against H3K9me². IgG was used as a negative control for the IP (n=2 replicates). **(C)** *RPTOR* mRNA levels at indicated time points after the addition of 150μM DFO. Samples matched with Figure 4D. Internal control: *POLR2A* (n=4 replicates per condition, one-way ANOVA and Tukey's post-hoc test, mean ± SE). **(D)** Immunoblot of *RPTOR*, mTOR and HIF1-α levels in HEK293T cells treated with 100 μg/ml cycloheximide (CHX) for indicated time points. HIF1-α, which is rapidly turned over under normoxic conditions via the actions of the EGLN and Von-Hippel Lindau (VHL) proteins, was used as a positive control. **(E)** Immunoblot of mTORC1 activity and complex member RAPTOR in A549 cells after treatment with 150μM DFO for 48 hours. **(F)** Immunoblot of lysates from cells transfected with FLAG-RAP2A or FLAG-mTOR and treated with or without 150μM DFO for 48 hours. Immunoprecipitation was performed with anti-FLAG antibody. RAP2A = negative control. **(G)** Summary of IP studies in Panel F (n=3 replicates, unpaired t-test, mean ± SE). **(H)** Immunoblot of mTORC1 activity in WT and *NPRL2* KO HEK293T treated with and without 150μM DFO for 48 hours.

Figure S15. ID is an abiotic stress in *Arabidopsis thaliana* and represses *TOR1/KOG1* transcription rate in *Saccharomyces cerevisiae*.

(A) *A. thaliana* root growth on MS medium containing 0 (Control) or 400 μ M BPD for 4 days. Seedlings were transferred 5 days after stratification on BPD-free MS medium. (B) Summary bar graph of root length in panel A. Starting root length (white bar) and new root growth over 4 days (red bar) (n=18-24 replicates per condition, unpaired t-test, mean \pm SE). (C) Transcriptional rate of *TOR1*, *TOR2* and *KOG1* within 180 minutes of iron chelation in *S. cerevisiae* (n=3 replicates per condition, one-way ANOVA and Tukey's post-hoc test, mean \pm SE, (*) = $P < 0.05$ for *TOR1*, (†) = $P < 0.05$ for *KOG1*).

Figure S16. The Jumonji-C KDM family inhibitor IOX1 mimics the actions of ID on mTORC1 activity and leucine uptake, and loss of *NPRL2* protects mTORC1 activity from suppression by IOX1.

(A) RT-PCR of AA transporters, *RPTOR* and *TTP* in HEK293T cells treated with various Jmj-C domain inhibitors for 12 hours. Internal control: *POLR2A* (n=3-4 replicates per condition mean \pm SE). (B) Immunoblot of mTORC1 activity and H3K9me² levels in A549 cells treated with 150 μ M DFO or 250 μ M IOX1 for 18hrs. (C) Immunoblot of indicated proteins in A549 cells treated with 250 μ M IOX1 for 48 hours. (D) Immunoblot of cytosol and membrane fractions from HepG2 cells treated with 250 μ M IOX1 for 12 hours. (E) Densitometry summary of data in Panel D (n=3 replicates per condition, unpaired t-test, mean \pm SE). (F) ¹⁴C-leucine uptake into HEK293T cells treated with 150 μ M DFO or 100 μ M IOX1 for 18 hours (n=5-6 replicates per condition, one-way ANOVA and Tukey's post-hoc test, mean \pm SE). (G) ¹⁴C-leucine uptake into HeLa cells treated with 150 μ M DFO or 100 μ M IOX1 for 18 hours (n=5-6 replicates per condition, one-way ANOVA and Tukey's post-hoc test, mean \pm SE). (H) Immunoblot of mTORC1 activity WT and *NPRL2* KO HEK293T cells treated with 250 μ M IOX1 for 18 hours. (I) Quantification of immunoblot in panel H (n=3 replicates per group, one-way ANOVA with Tukey's post-hoc test. mean \pm SE).

Figure S17. H3K9 di-methyl ChIP-seq signal in iron chelated samples correlate with changes after loss of *KDM3A* and *KDM3B*.

(A) Heatmap of the log₂FC in H3K9me² signal between DFO treatment and control plotted against *KDM3A* and *KDM3B* occupancy. K-means cluster =3. (B) Browser tracks with *KDM3B* and H3K9me² track data from HCT116 cells treated with control shRNA (shC) or shRNA targeting *KDM3A* and *KDM3B* (sh3A3B). Track data for *KDM3A* was downloaded from the GEO database accession GSE127624. Track data for *KDM3B* and H3K9me² from HCT116 cells were downloaded from the GEO database accession GSE71885. (C) Hierarchical clustering and correlation analysis between indicated samples using deepTools plotCorrelation. Values indicate the Pearson correlation between the sample listed in the corresponding row and column.

Figure S18. CRISPR-mediated deletion of *KDM3A*, *4B*, or *4C* does not protect mTORC1 activity during ID, and *KDM3B* KO cells have increased cell death during ID.

(A) Immunoblot showing deletion of *KDM4A* and *4B*, using CRISPR-Cas technology in HEK293T cells. (B) Immunoblot of mTORC1 activity and H3K9me² in Cas9 (WT) and *KDM3A*, *KDM4B* or *KDM4C* KO HEK293T cells in the presence and absence of 150 μ M DFO for 18 hours. (C) Immunoblot of mTORC1 activity and H3K9me² in HEK293T cells with overexpression of HA-tagged *KDM4A*, *KDM4B* or combination of the two proteins treated with 150 μ M DFO for 18 hours. (D) Immunoblot of mTORC1 activity and H3K9me² in Cas9 (WT) and sg.3B c.7 (*KDM3B* KO) TSC2 KO HeLa cells in the presence and absence of 150 μ M DFO for 18 hours.

(E-F) Summary of immunoblot in panel D (n=3 replicates per group, one-way ANOVA with Tukey's post-hoc test. Mean \pm SE). **(G)** Fluorescent microscopy of cell death using Hoescht and propidium iodide (PI) double staining in *KDM3B* KO HEK293T cells treated with 150 μ M DFO for 0, 24, 36 and 60 hours **(H)** Quantification of images in panel G. (n=6 replicates, one-way ANOVA and Tukey's post-hoc test, mean \pm SE).

Figure S19. The oxygen-sensor KDM6A has a high affinity for iron, and marker of tumor iron status influences survival and correlates with expression of KDM3B and mTORC1 related genes.

(A) SDS-PAGE gel of purified N-terminal FLAG-tagged WT KDM6A and KDM6A^{MT/ED} mutant expressed using a baculoviral overexpression system. **(B, C)** Enzyme kinetics of WT KDM6A **(B)** and KDM6A^{MT/ED} **(C)** in the presence of increasing concentrations of iron. **(D)** Enzyme kinetics of KDM3B in the presence of increasing concentrations of R-2HG. **(E)** Immunoblot of mTORC1 activity in HEK293T cells after treatment with 150 μ M DFO or increasing concentrations of octyl-R-2HG. **(F)** Ordered list of tumor types by *TFRC* expression. **(G)** Cox-proportional hazard curves of overall survival in cancer patients stratified by median expression of *TFRC*, *PAT1*, and *RPTOR*. **(H)** Correlation between the expression of *LAT3*, *PAT1*, or *RPTOR* and *KDM3B* in *TFRC* over-expressing tumors.

Figure S20. ID increases cancer cell sensitivity to genotoxic chemotherapy, and represses RAPTOR levels and mTORC1 activity in patient-derived primary tumor cells.

(A-B) Quantification of viable A549 adenocarcinoma **(A)** and HeLa cervical carcinoma **(B)** cells after treatment with the indicated doses of Cisplatin for 48 hours in the presence and absence of 150 μ M DFO (n=6 replicates, one-way ANOVA and Tukey's post-hoc test, mean \pm SE). **(C)** Immunoblot of mTORC1 activity and RAPTOR expression in patient-derived primary tumor cells treated with 150 μ M DFO for the indicated times. **(D)** Summary of immunoblot in panel D (n=3 replicates per group, one-way ANOVA with Tukey's post-hoc test, mean \pm SE).

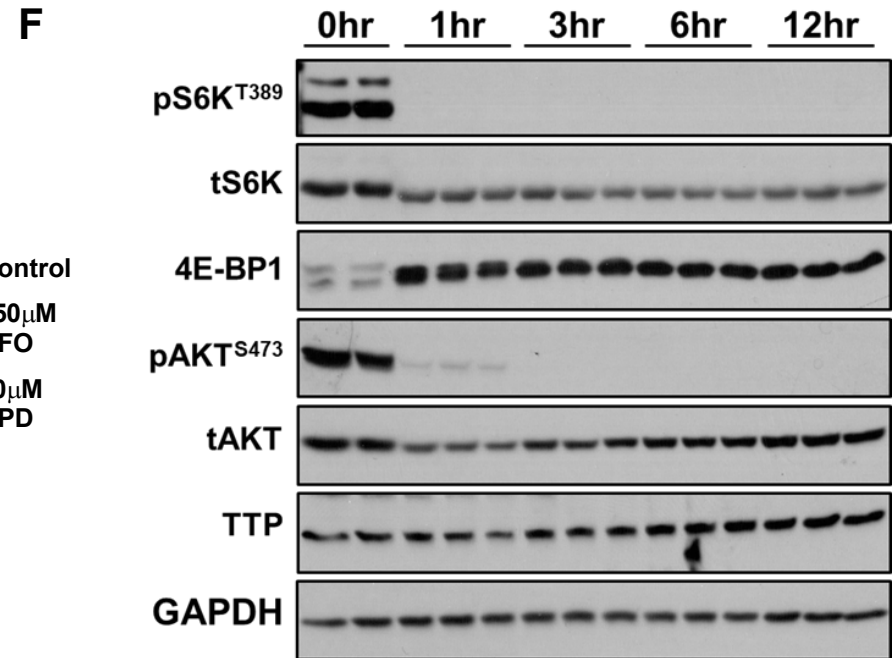
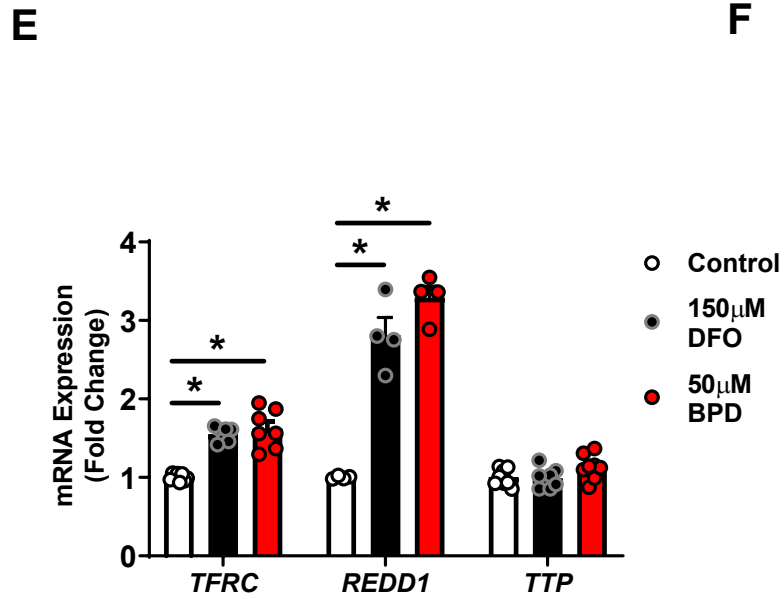
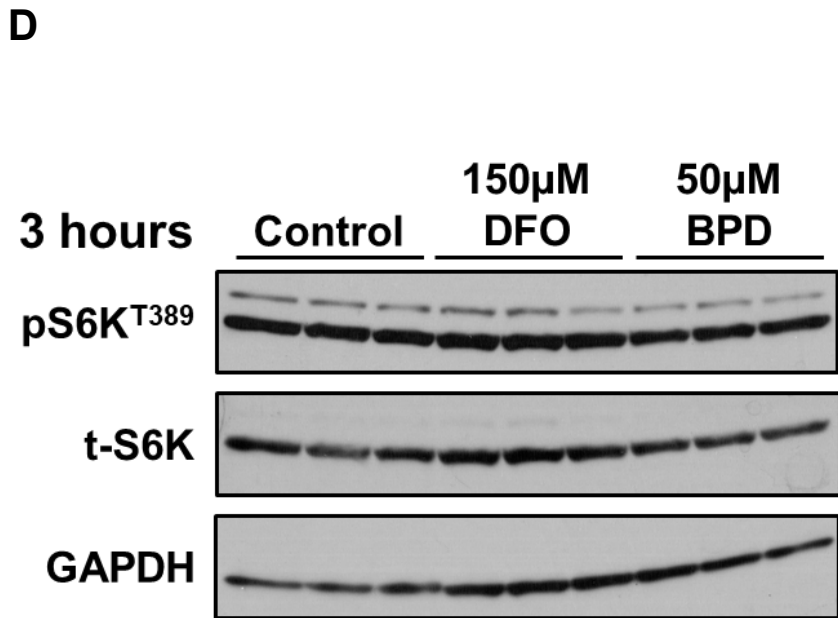
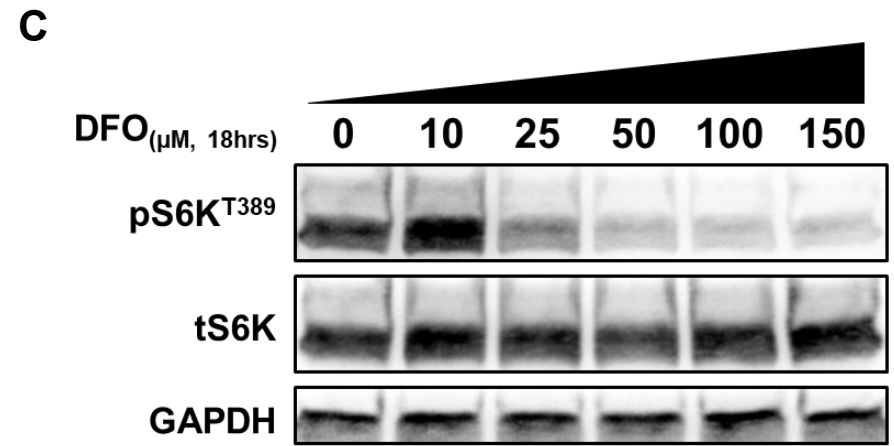
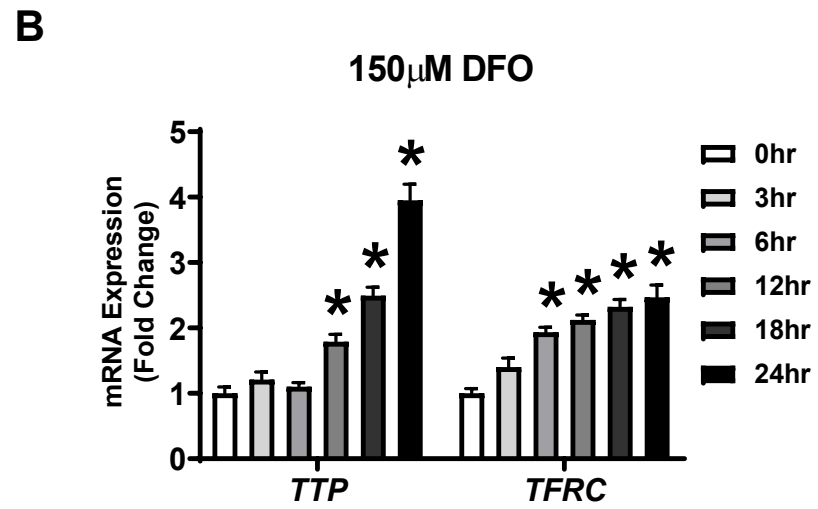
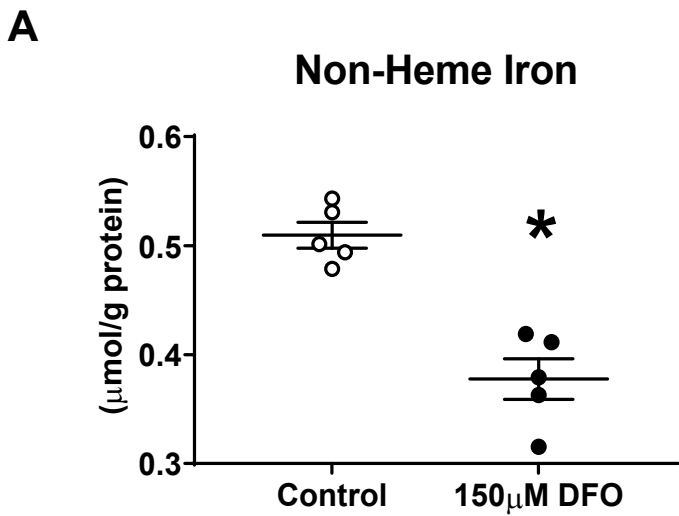


Figure S1

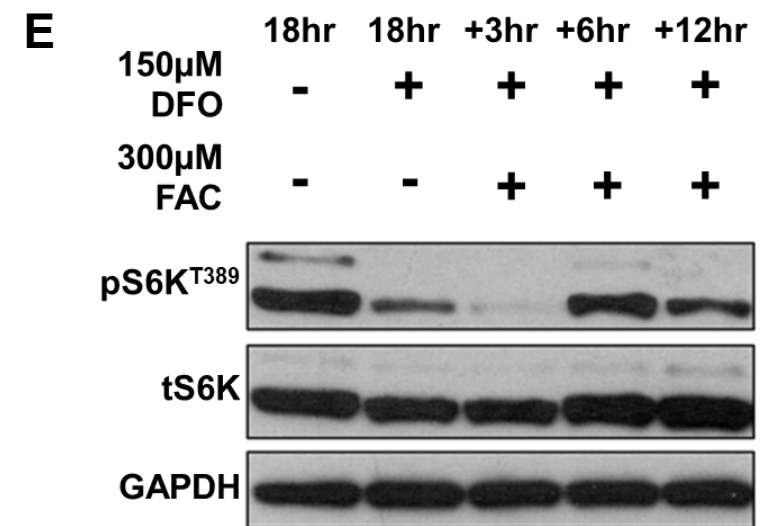
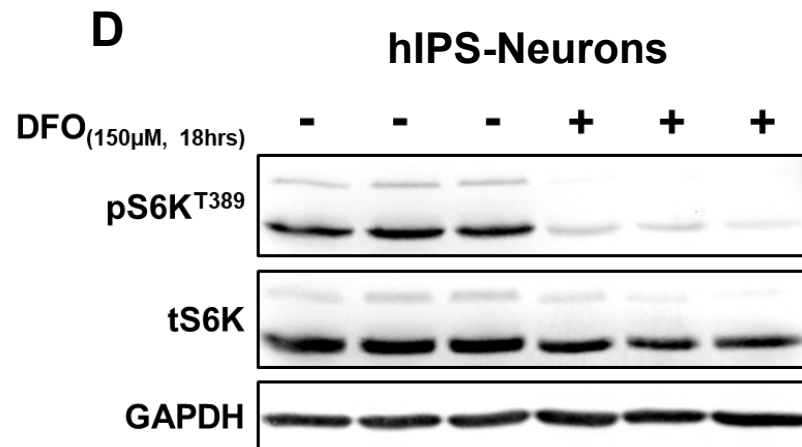
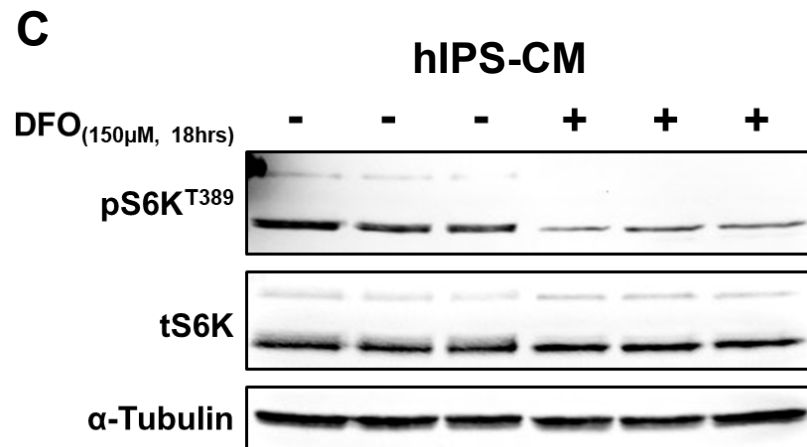
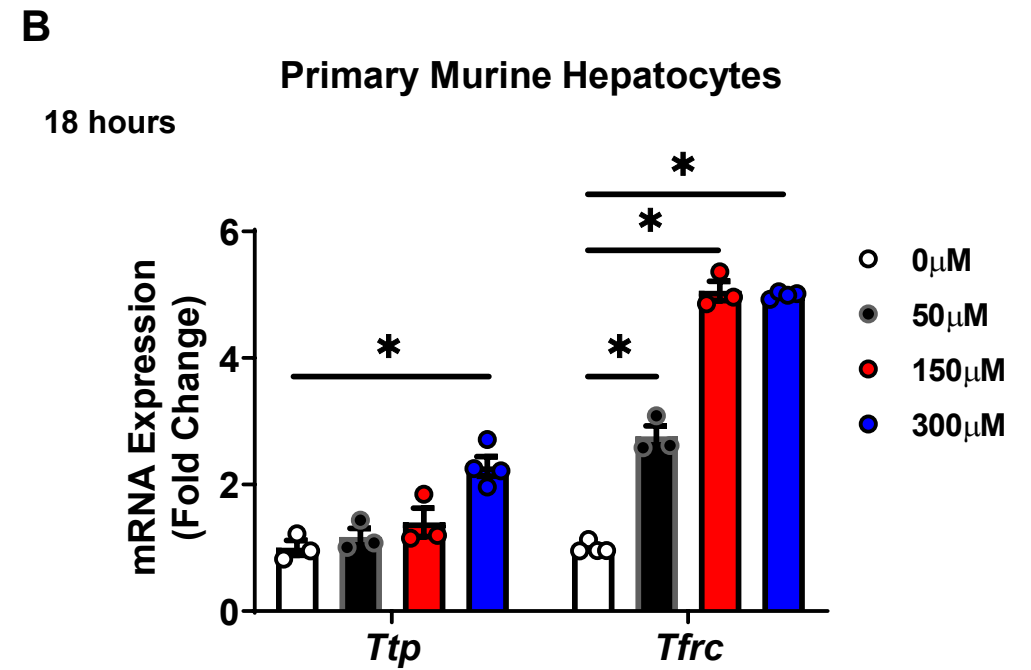
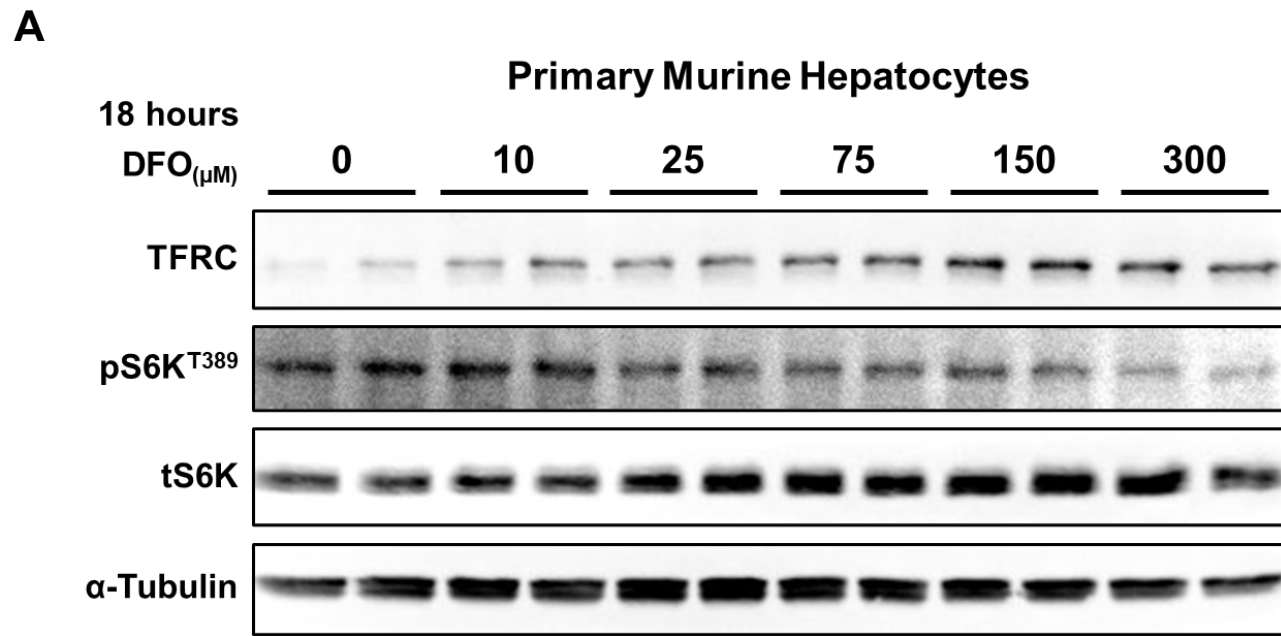
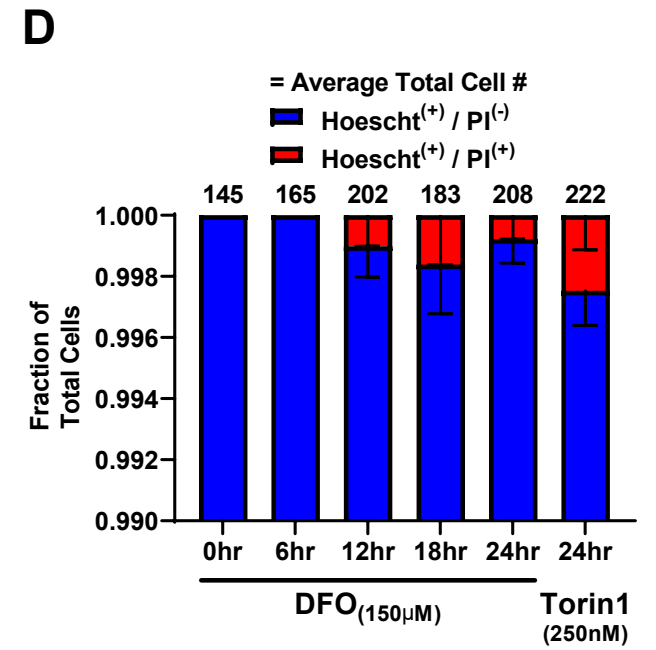
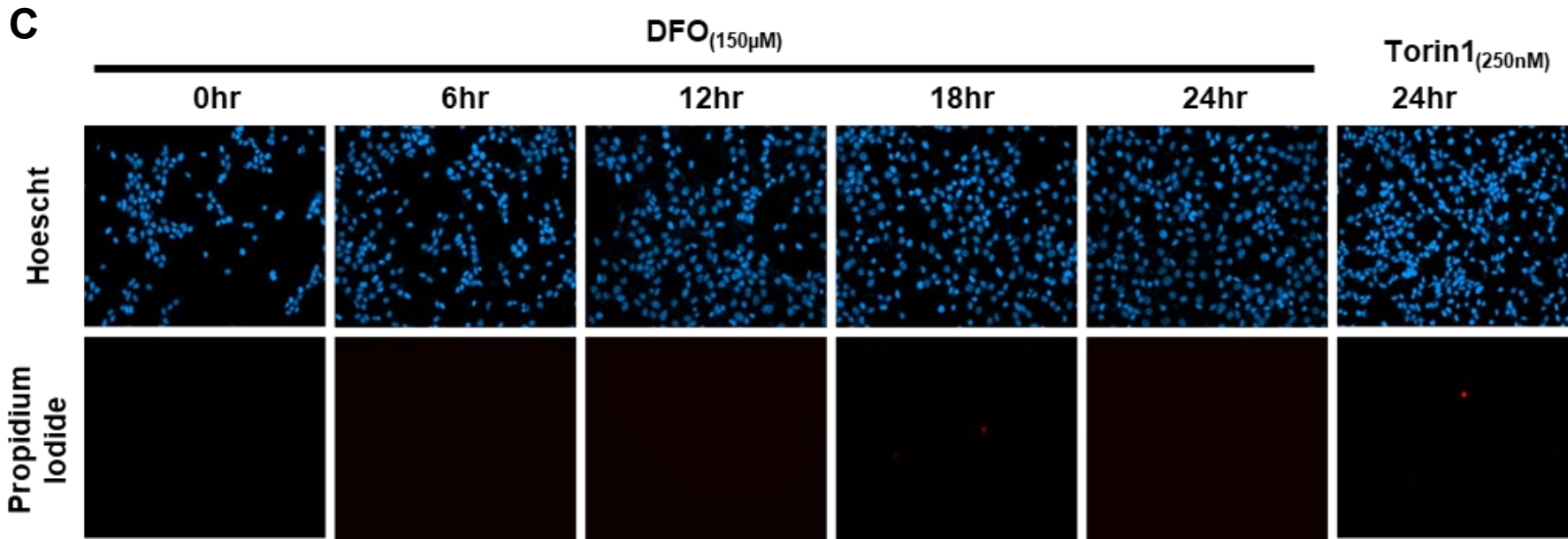
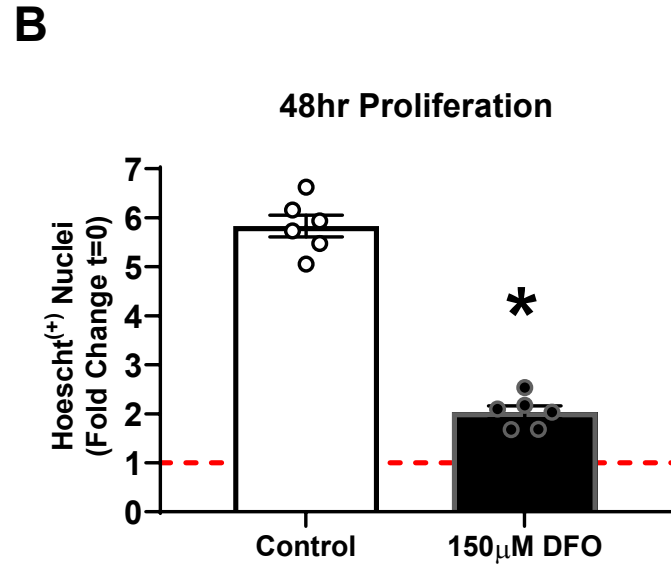
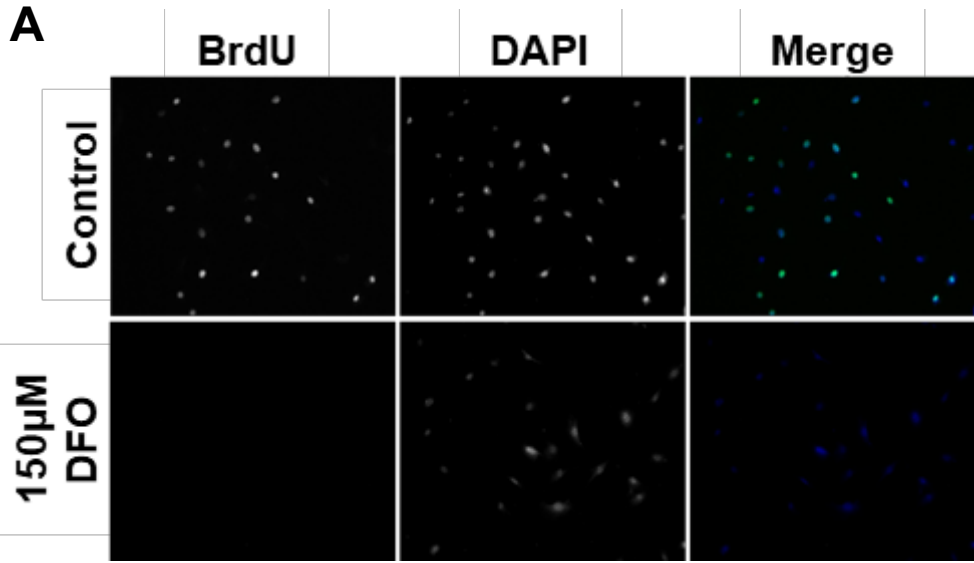


Figure S2

Figure S3



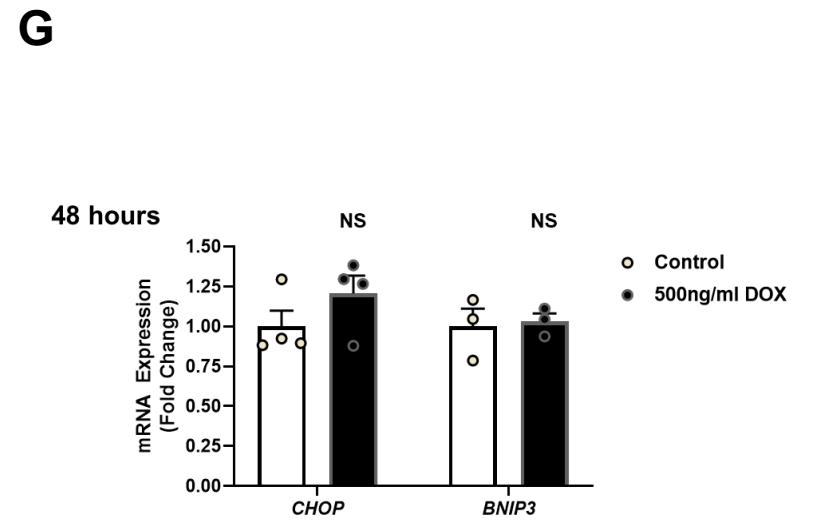
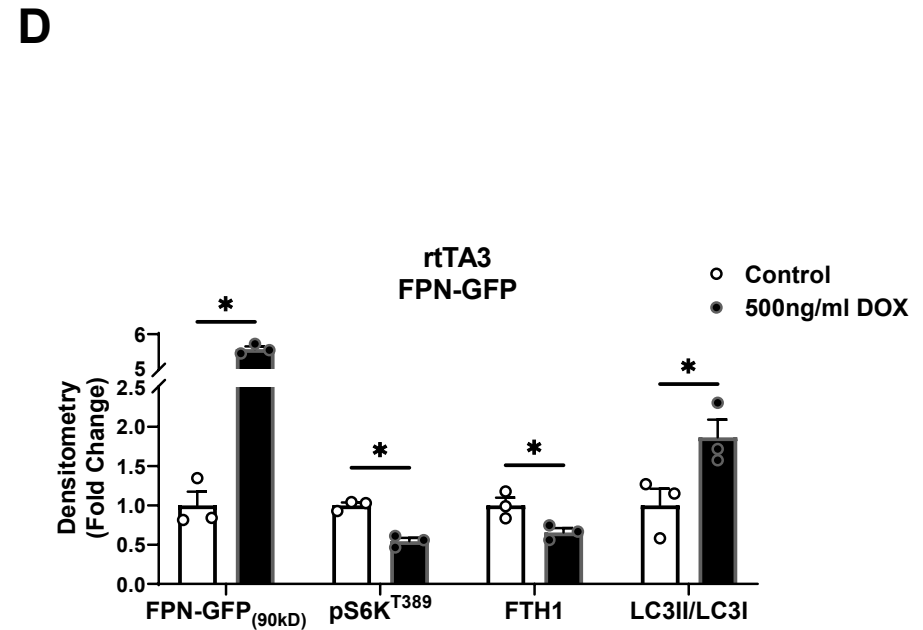
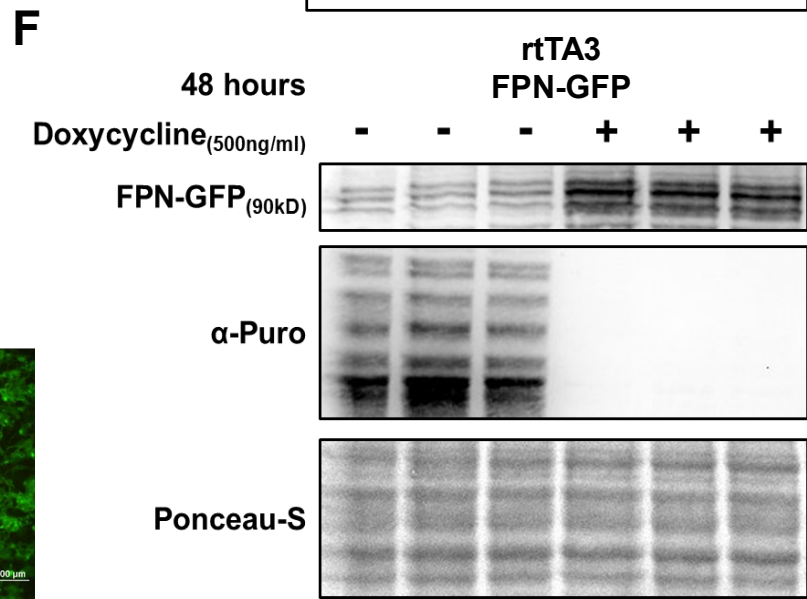
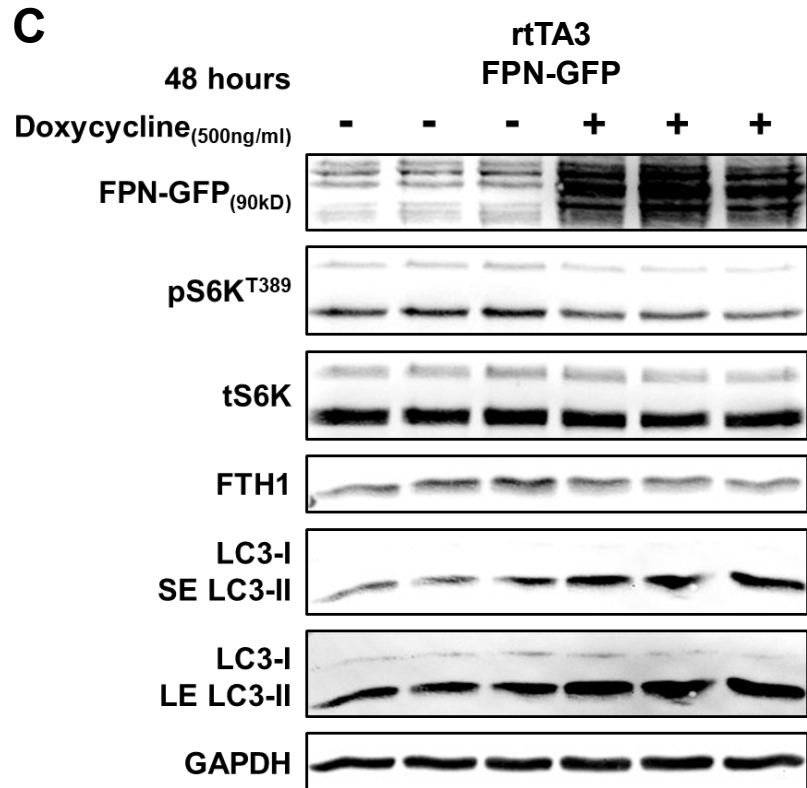
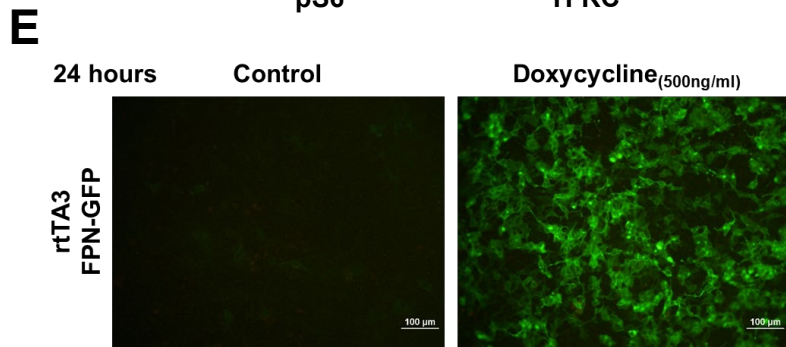
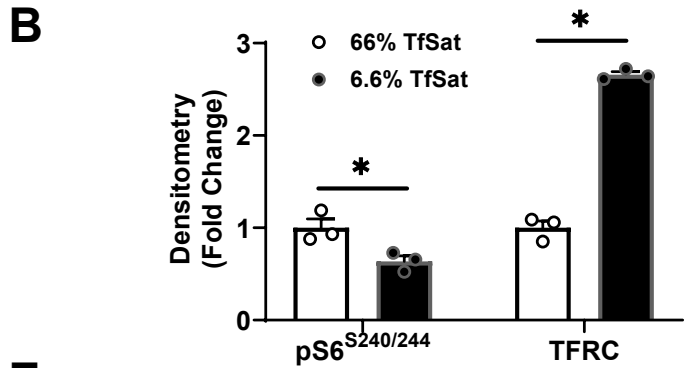
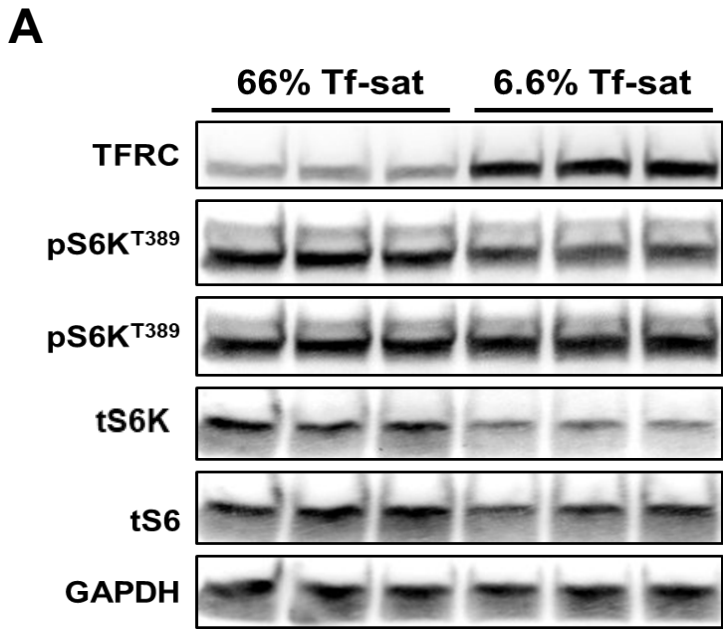


Figure S4

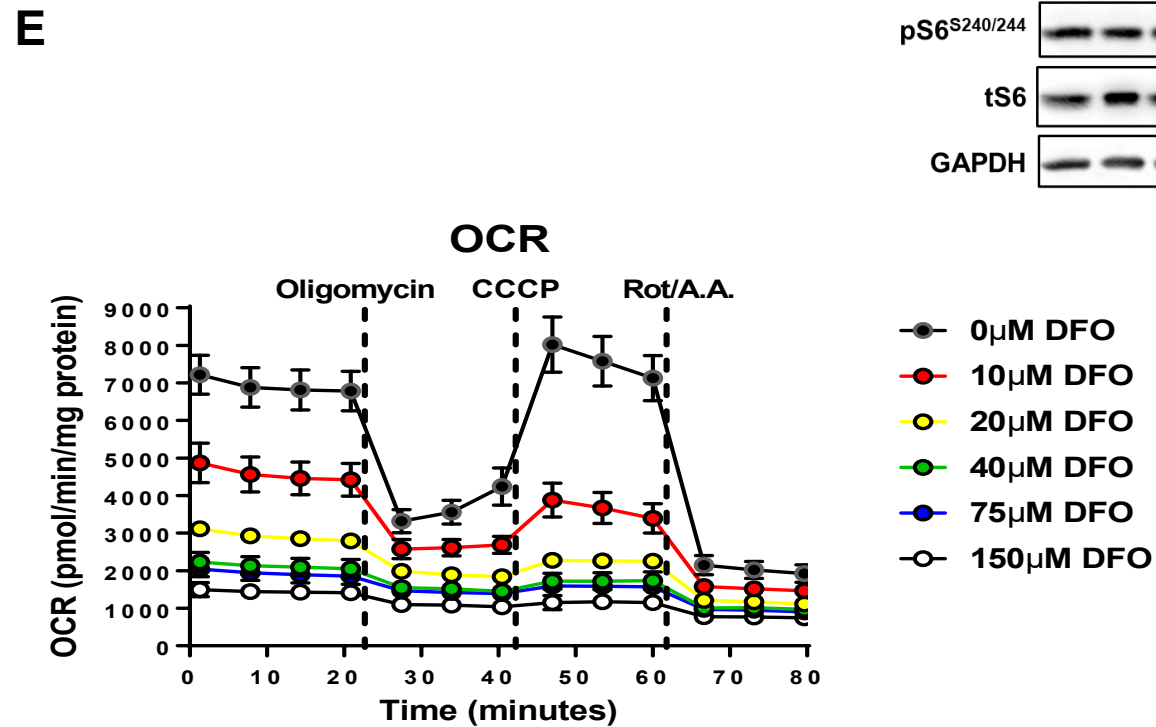
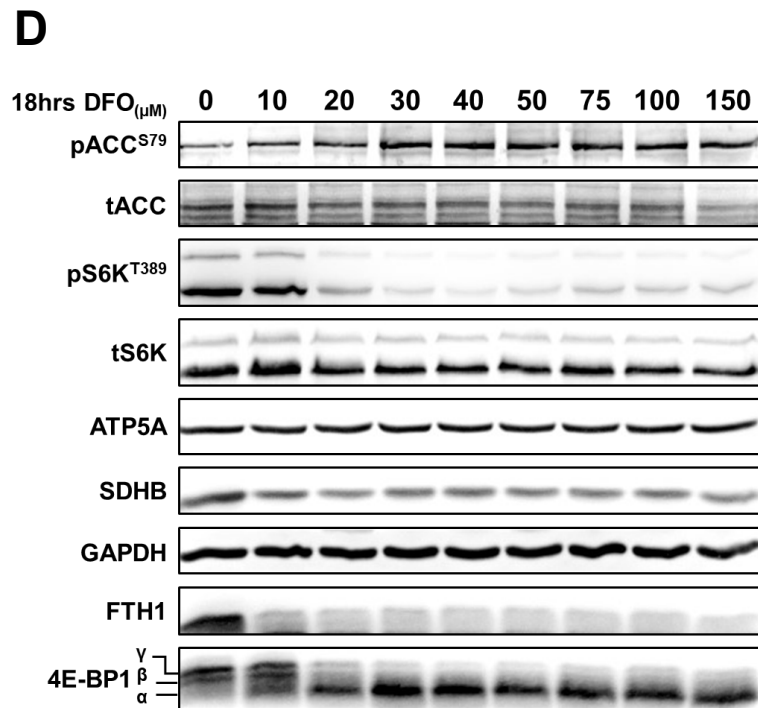
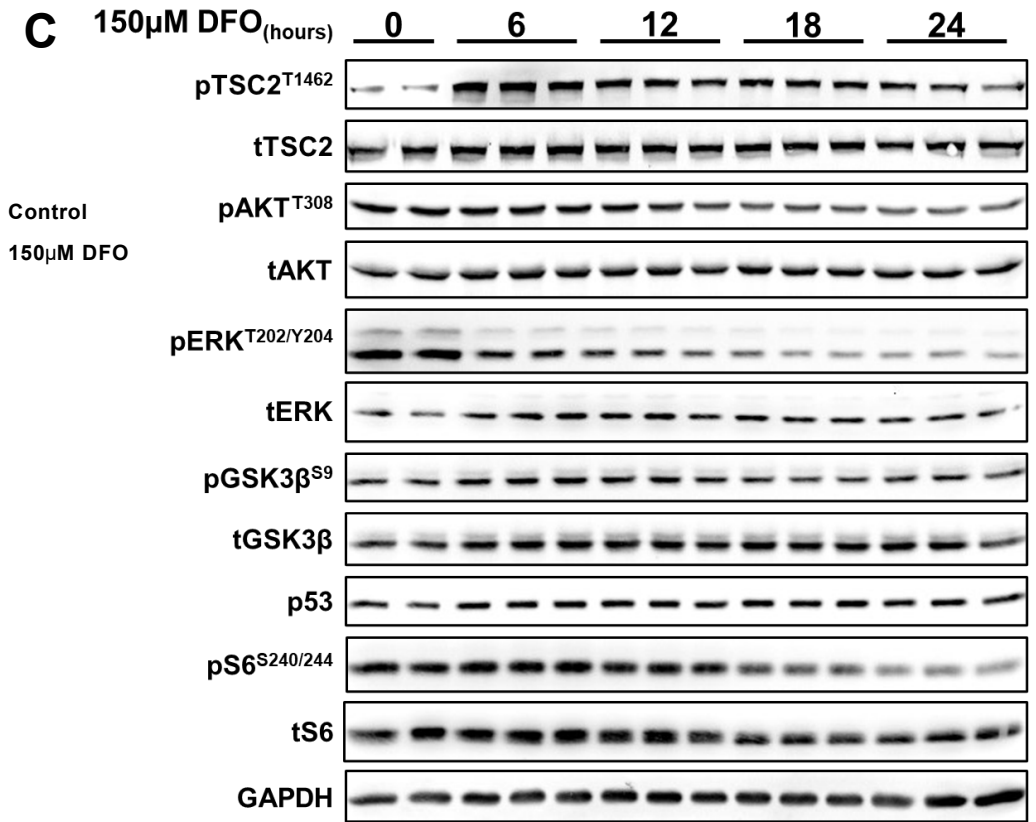
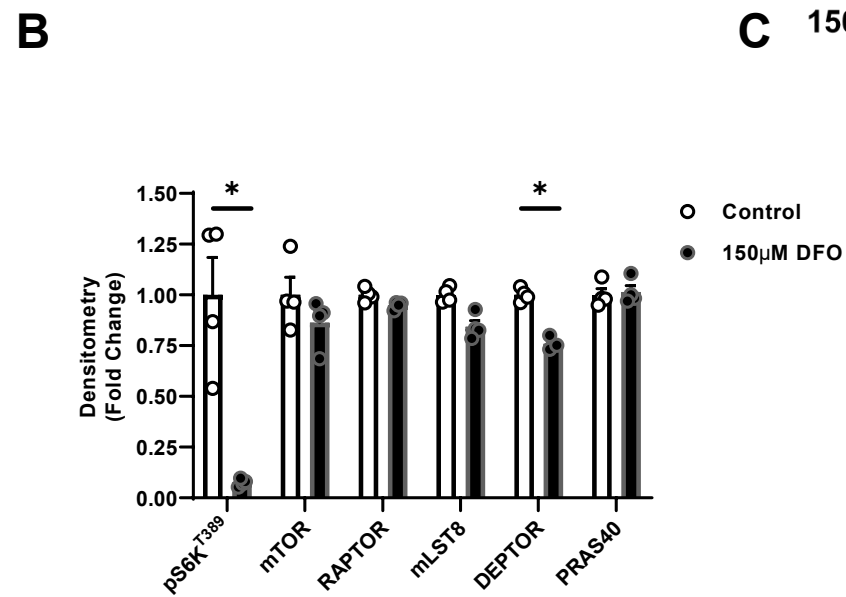
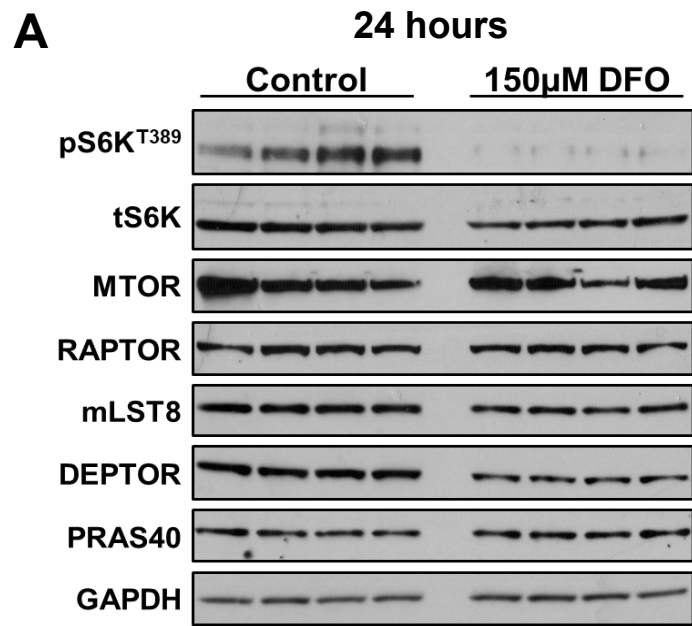
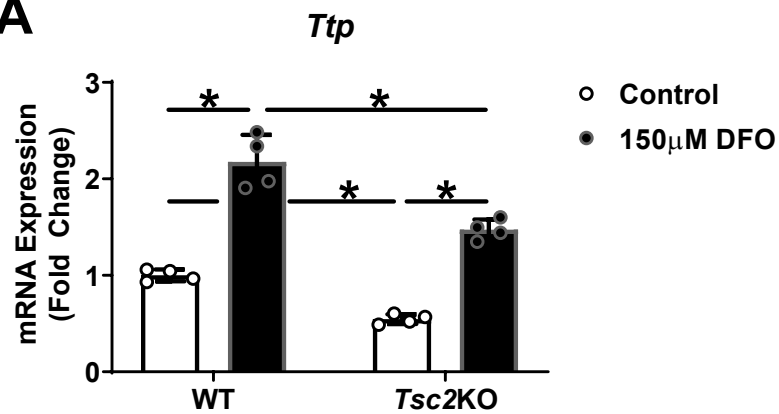
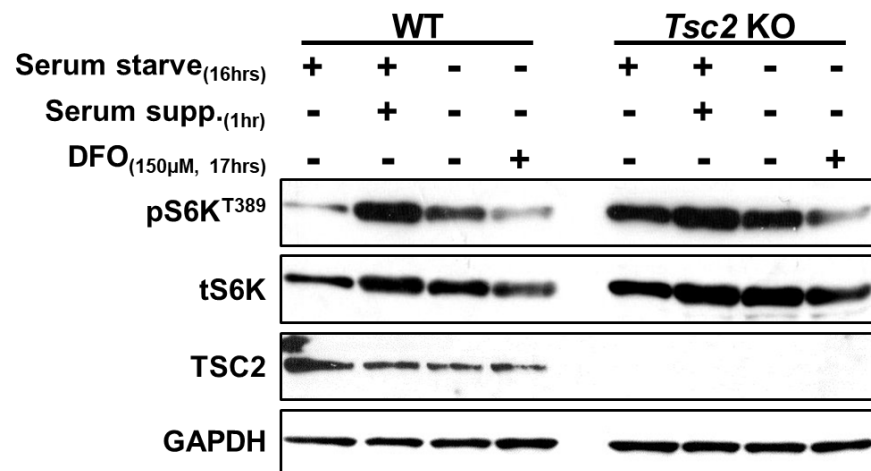
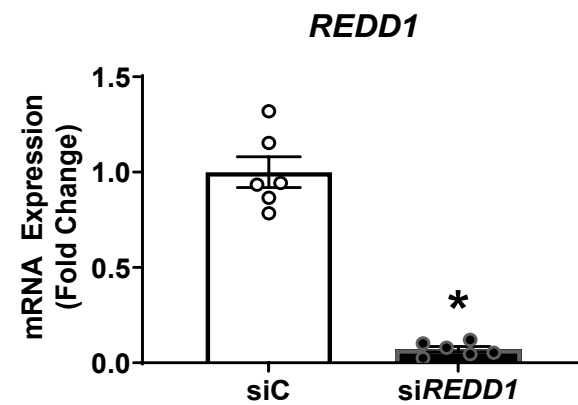
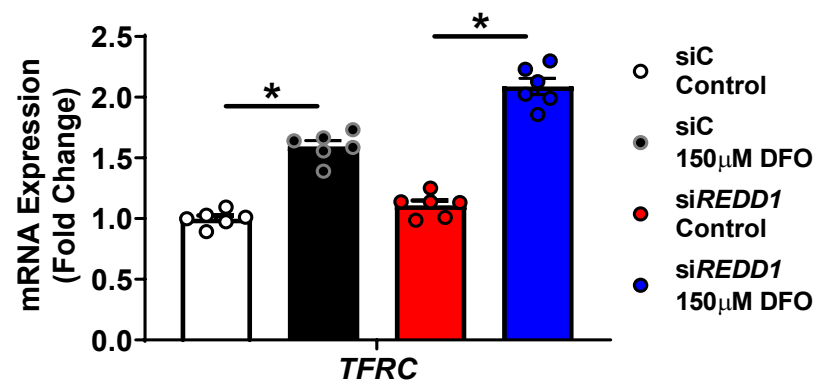
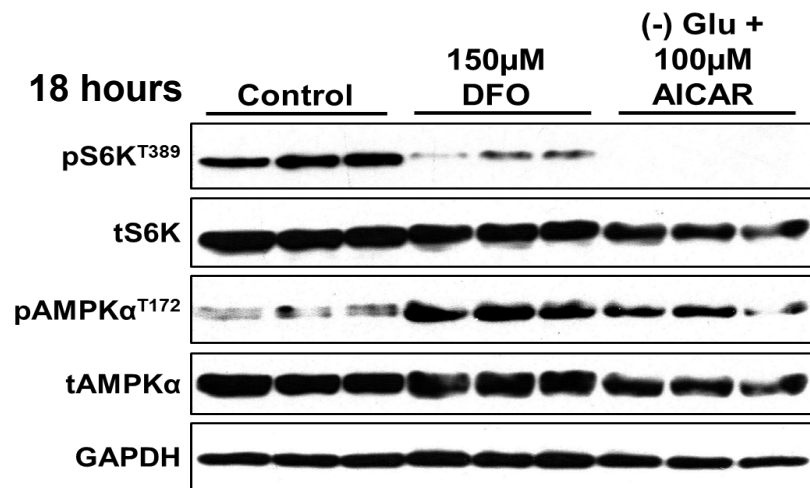
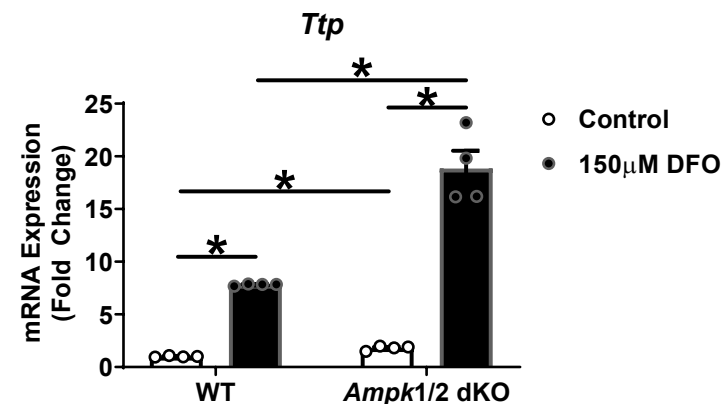
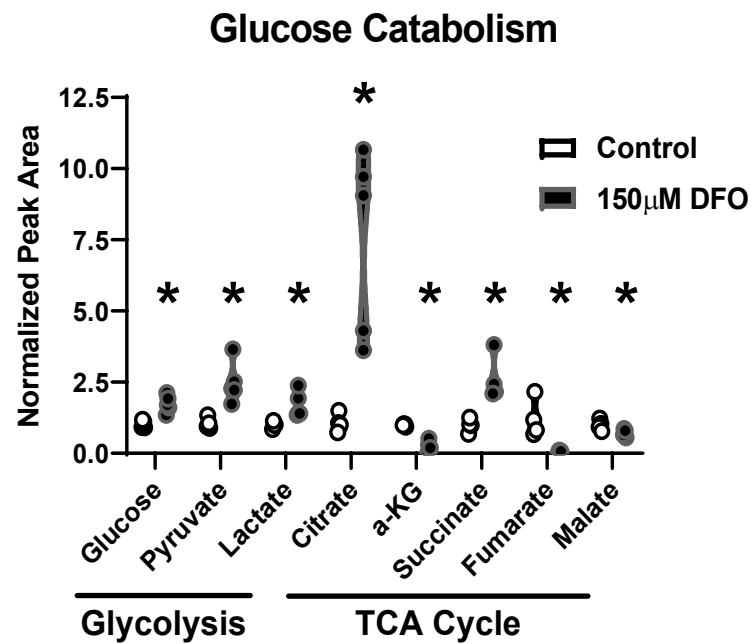
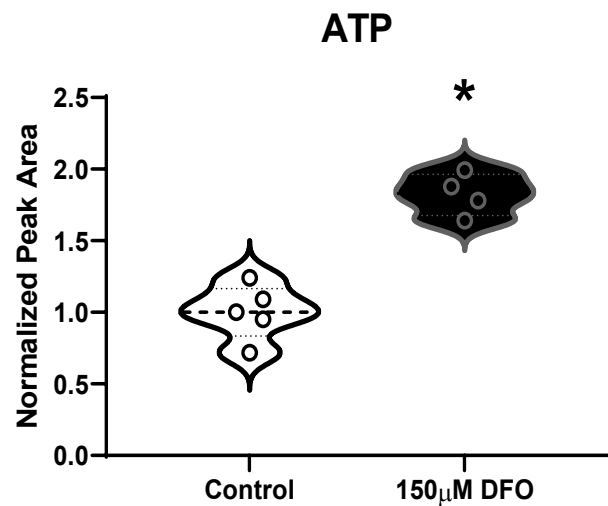
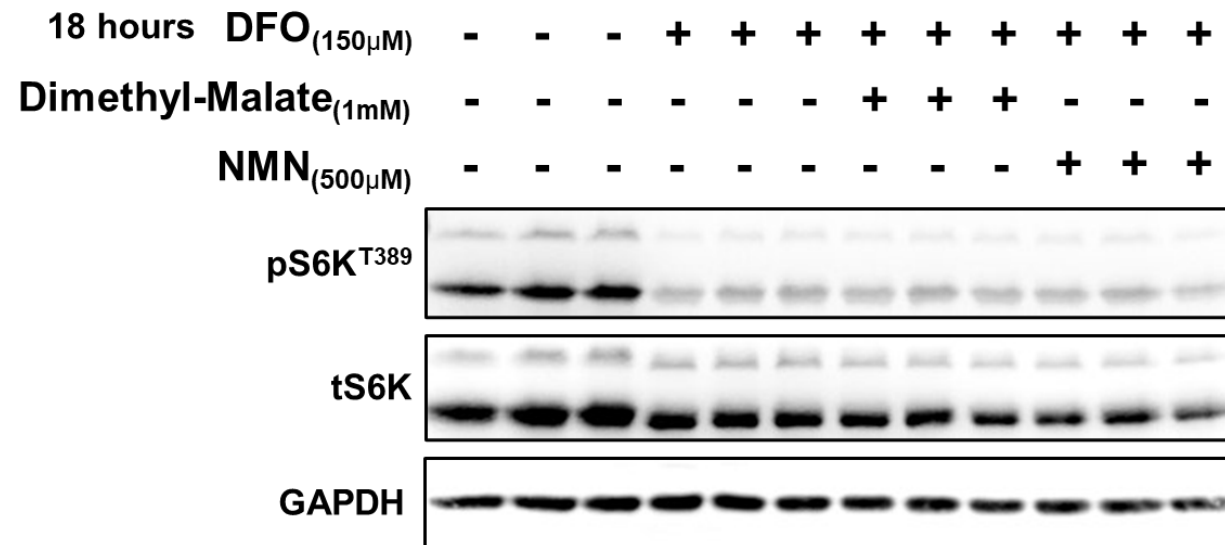
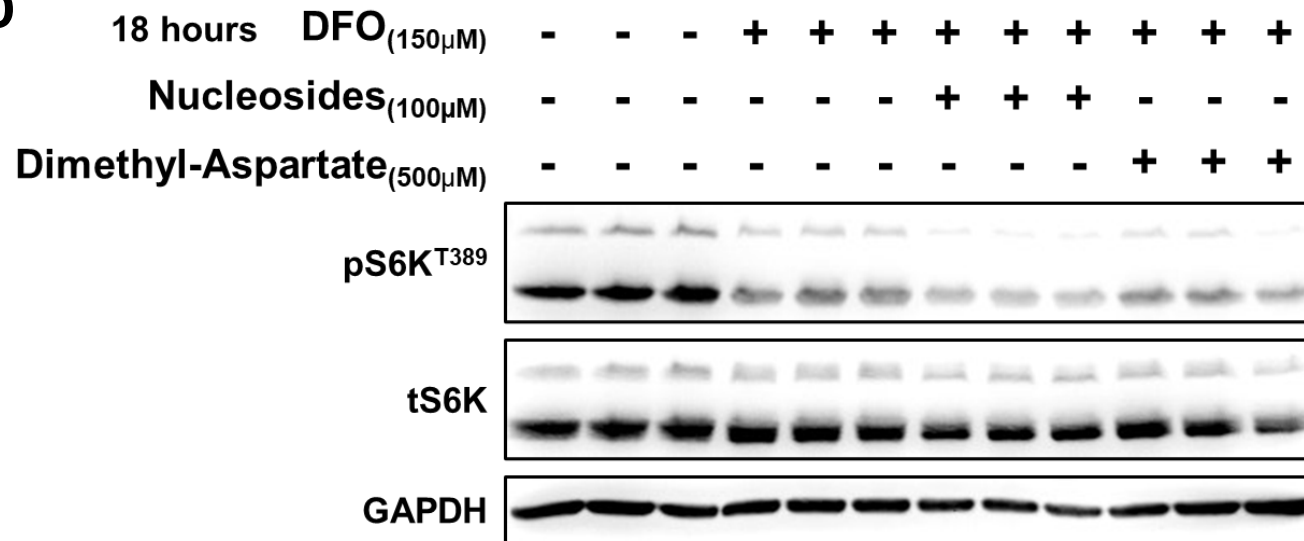
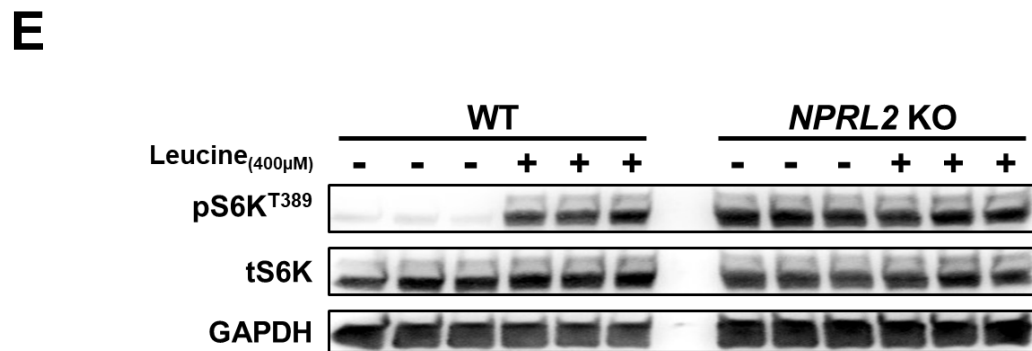
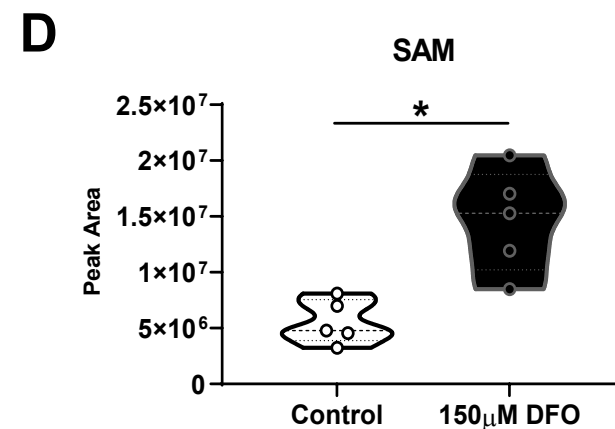
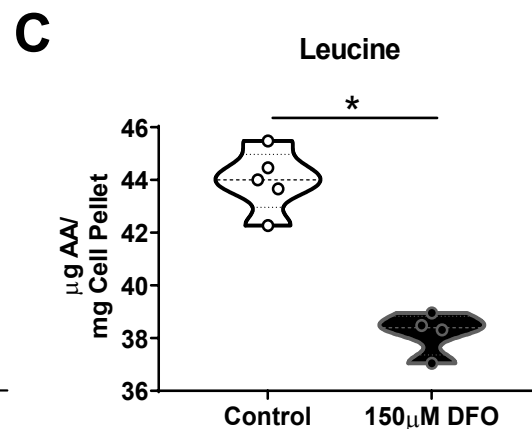
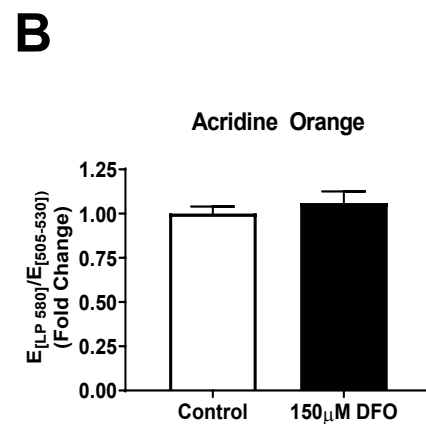
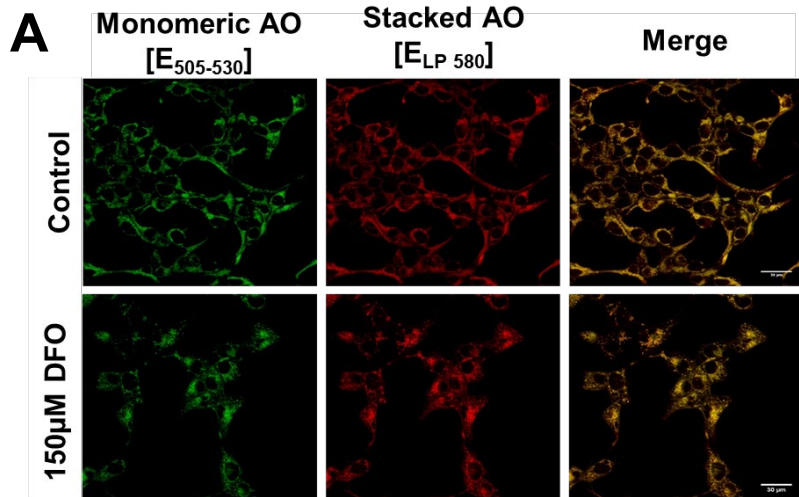


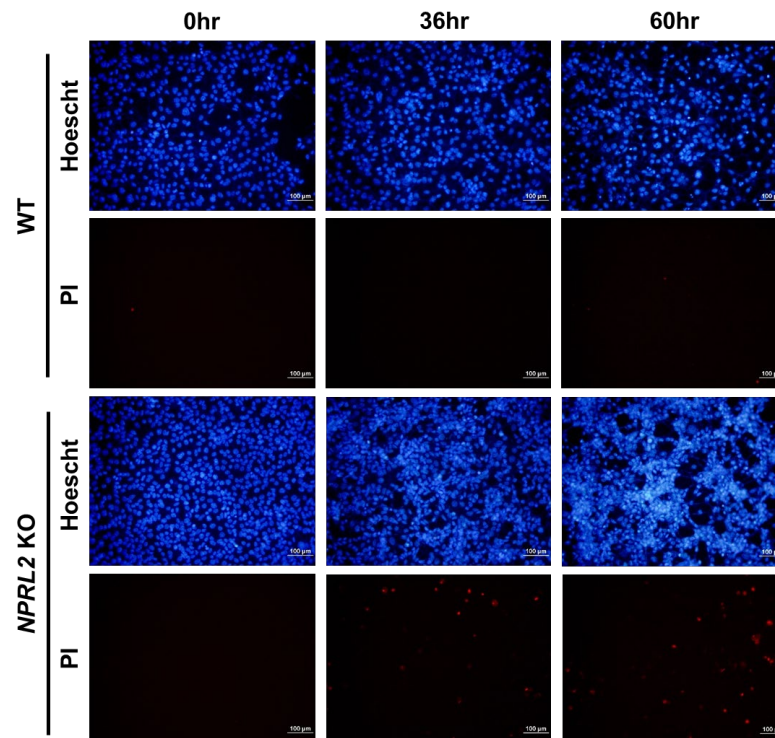
Figure S5

A**B****C****D****E****F****Figure S6**

A**B****C****D****Figure S7**



F



G

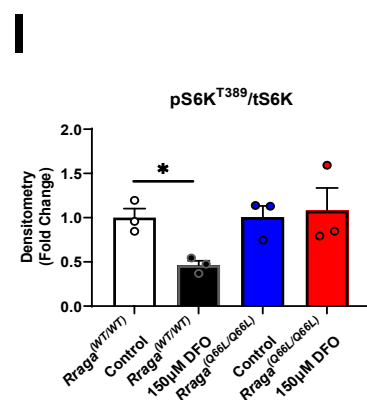
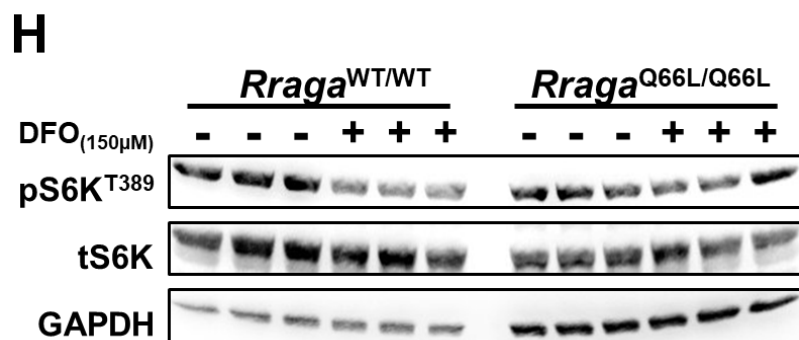
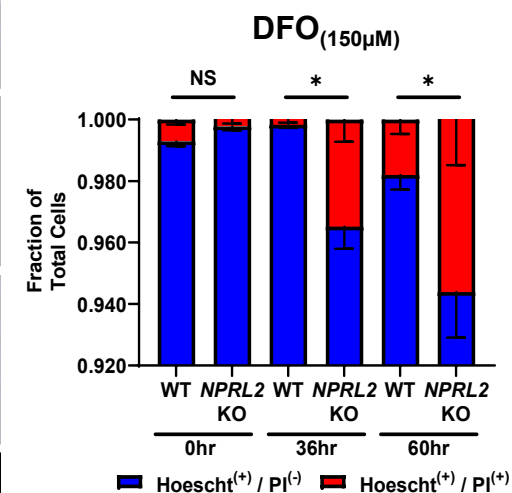


Figure S8

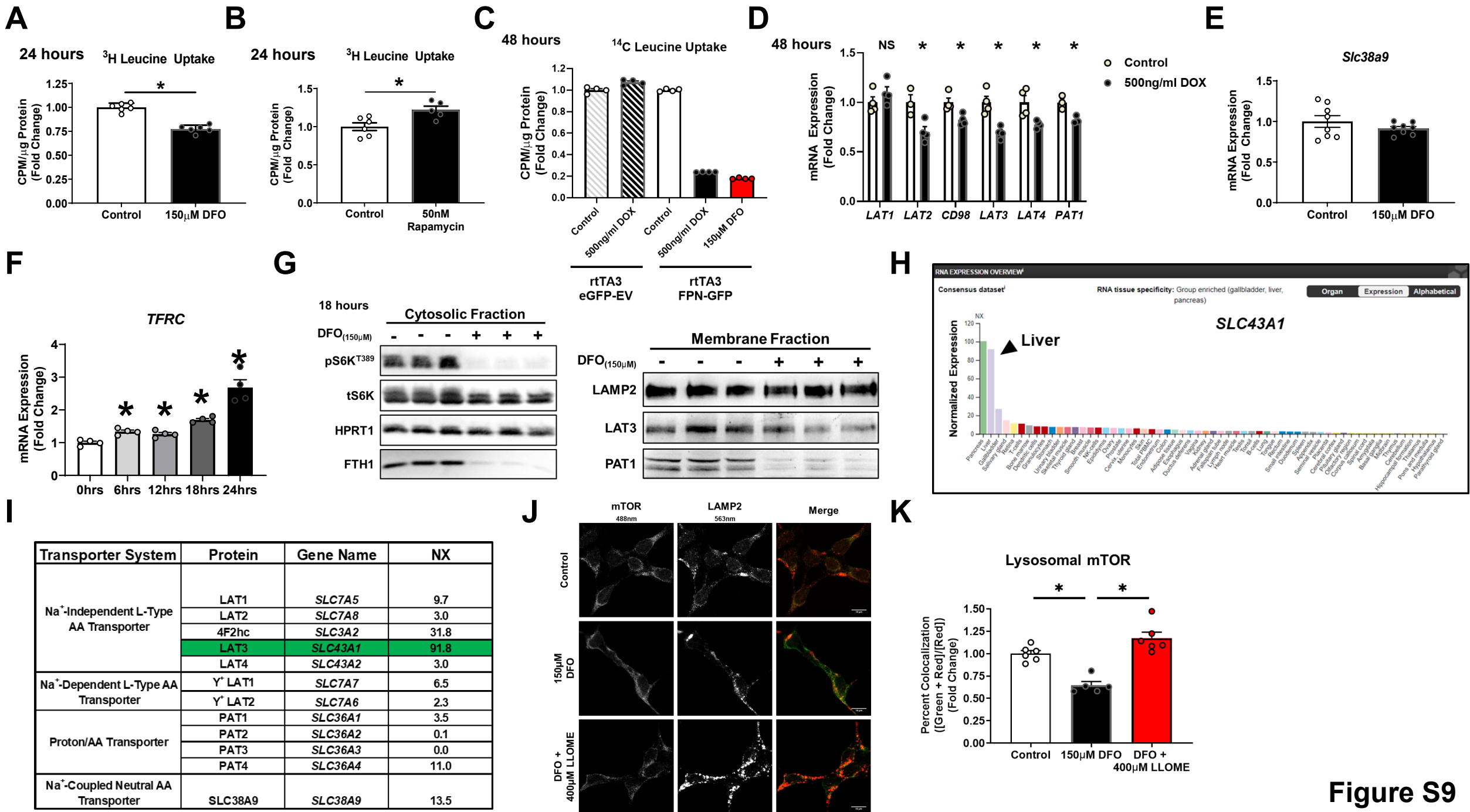
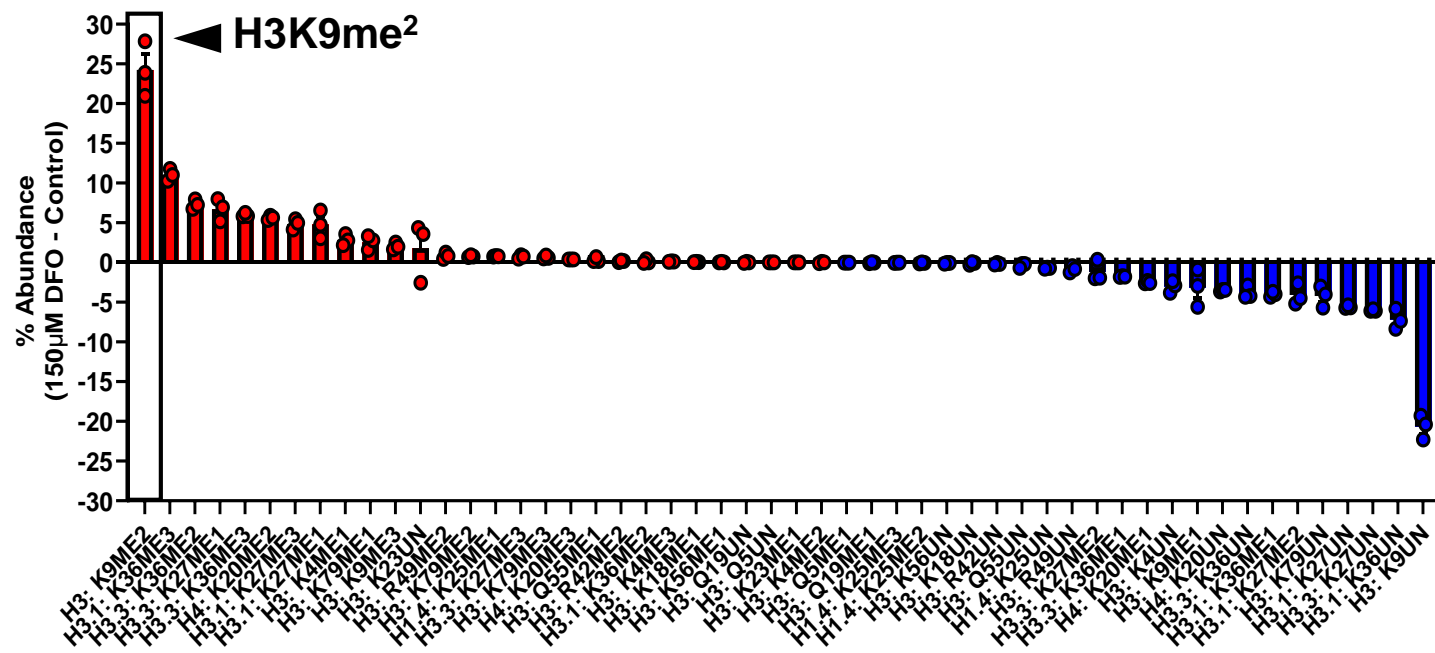
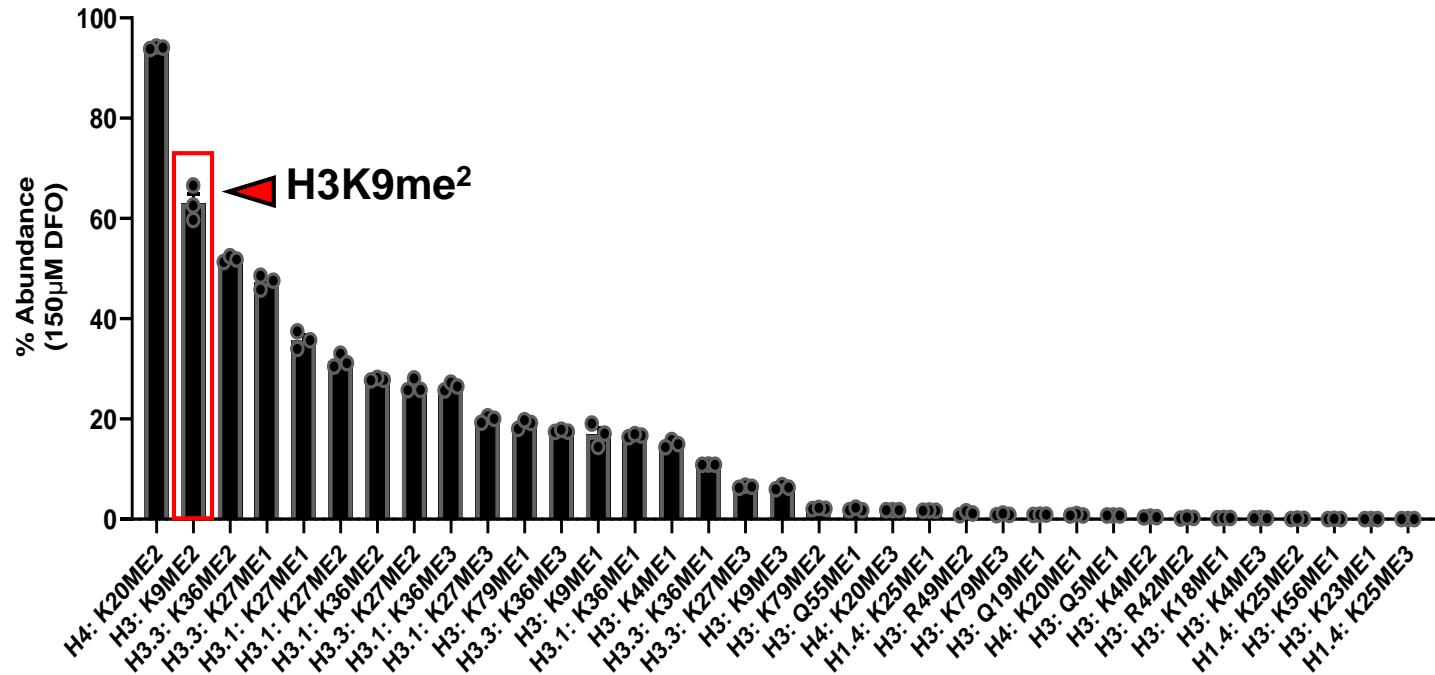


Figure S9

A**B****Figure S10**

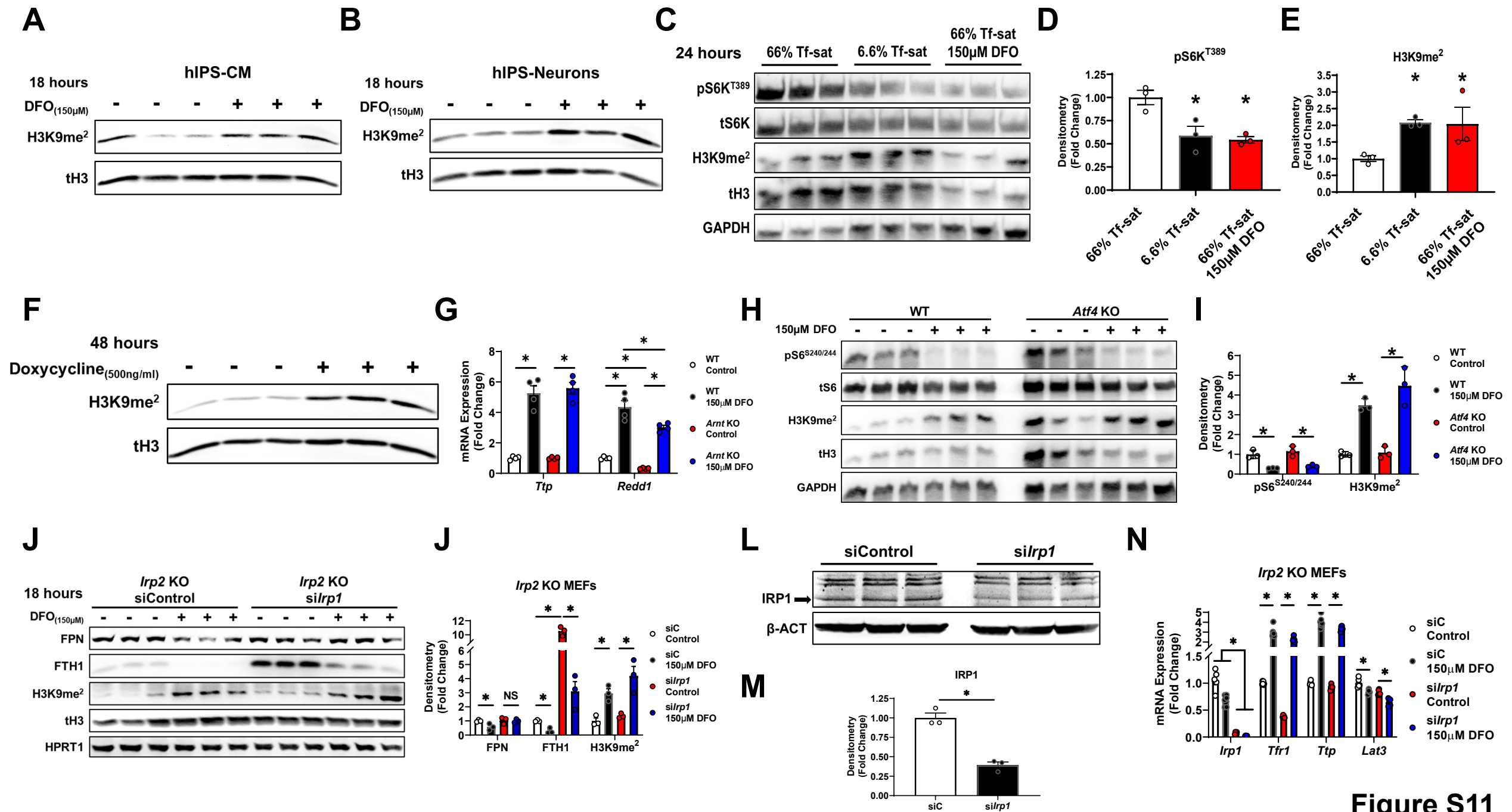


Figure S11

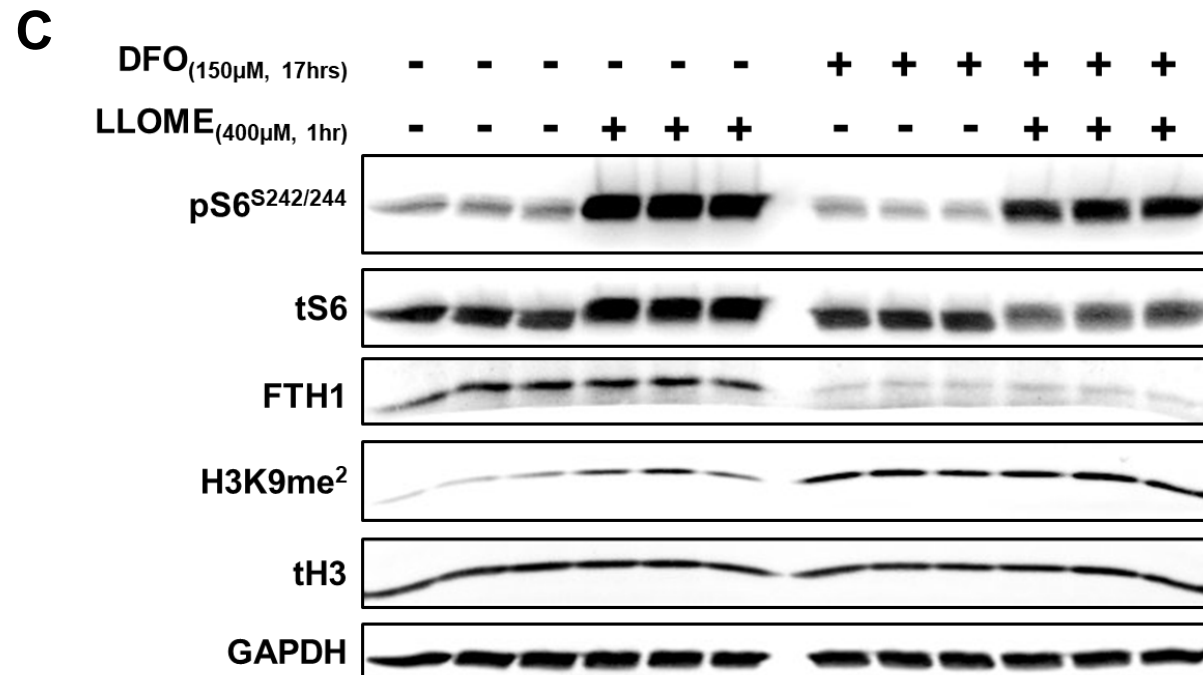
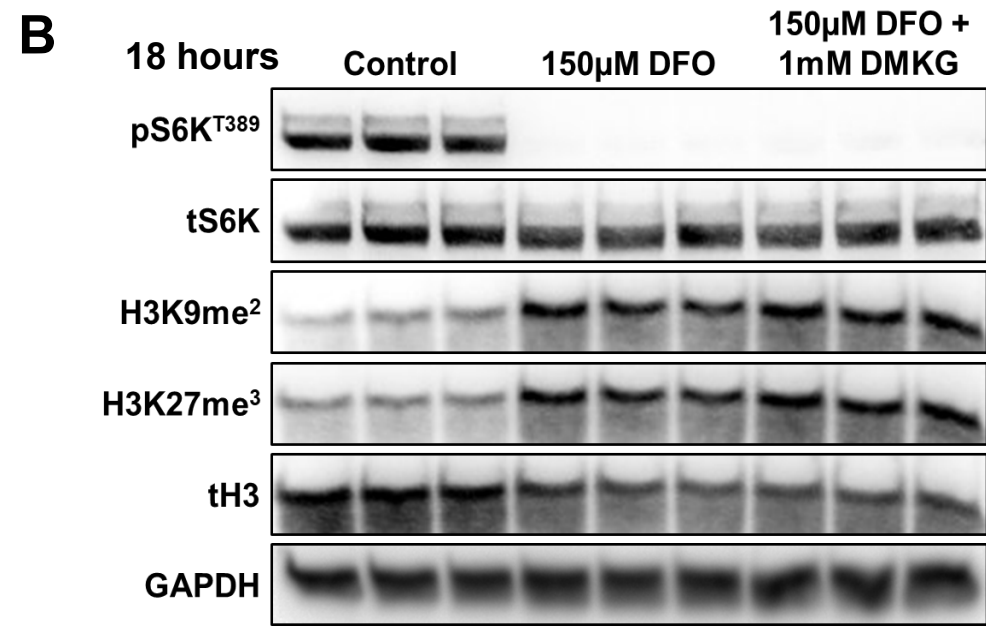
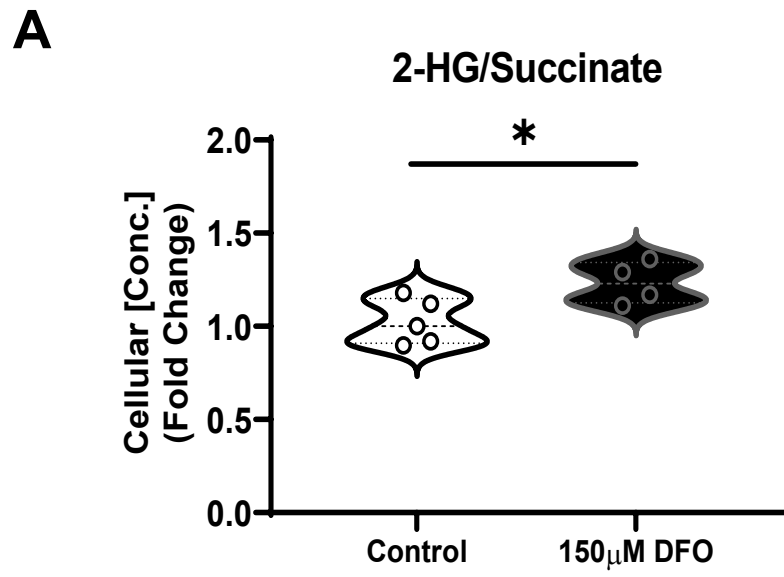
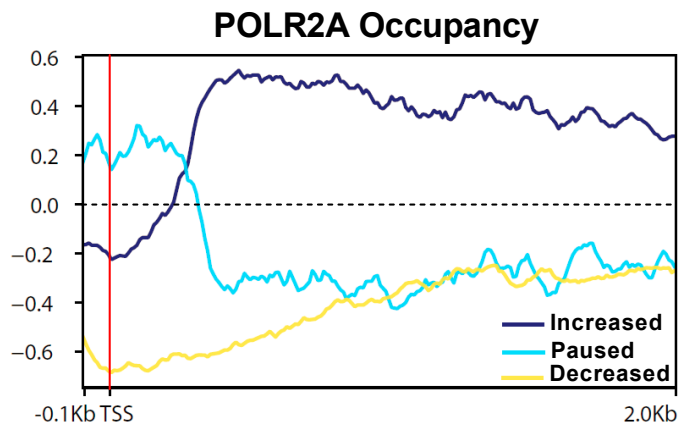


Figure S12

A



B

Increased

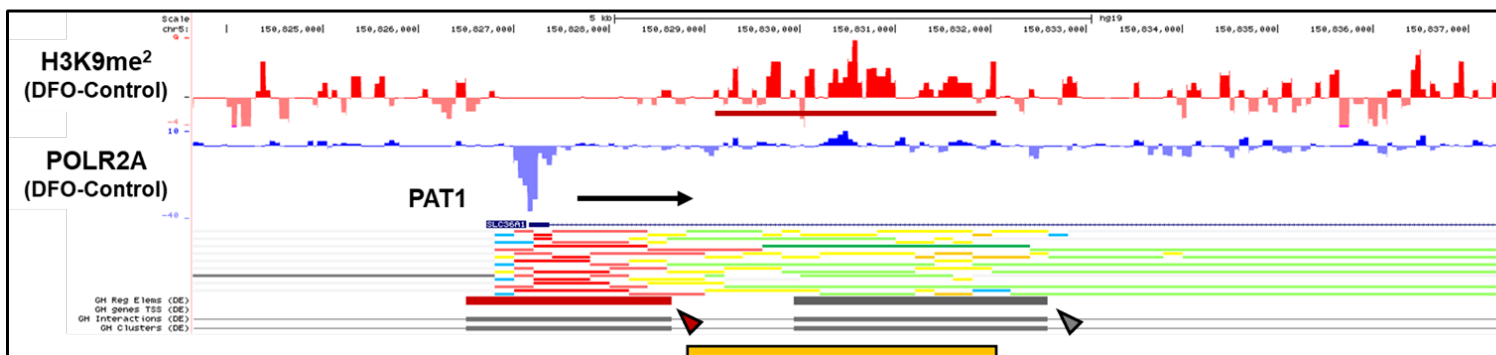
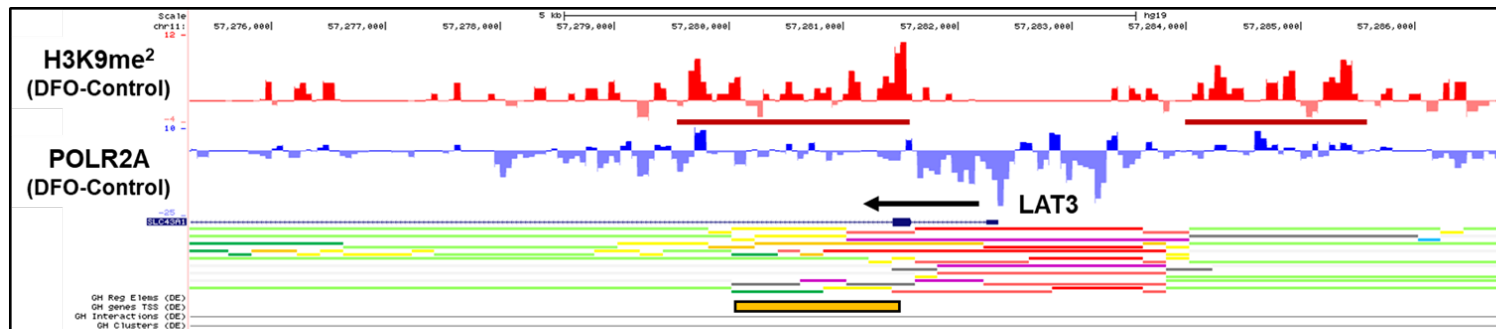
PANTHER GO - Biological Process	Fold Enrichment	FDR
carbohydrate transport (GO:0008643)	4.15	2.70E-02
activation of MAPK activity (GO:000187)	2.9	4.19E-02
positive regulation of I-kappaB kinase/NF-kappaB signaling (GO:0043123)	2.84	2.35E-02
cellular response to oxygen levels (GO:0071453)	2.7	2.30E-02
cellular response to decreased oxygen levels (GO:0036294)	2.66	3.87E-02
cellular response to hypoxia (GO:0071456)	2.66	4.97E-02
axon guidance (GO:0007411)	2.5	2.29E-02
neuron projection guidance (GO:0097485)	2.5	2.31E-02
response to oxygen levels (GO:0070482)	2.45	3.07E-03
response to hypoxia (GO:0001666)	2.33	2.30E-02
response to decreased oxygen levels (GO:0036293)	2.32	2.21E-02
axonogenesis (GO:0007409)	2.13	3.92E-02
cell morphogenesis involved in neuron differentiation (GO:0048667)	2.07	3.27E-02
chemotaxis (GO:0006935)	2.01	2.27E-02
taxis (GO:0042330)	2.01	2.30E-02

C

Decreased

PANTHER GO - Biological Process	Fold Enrichment	FDR
cytoplasmic translation (GO:0002181)	3.61	0.00239
cell-substrate adhesion (GO:0031589)	3.32	0.0145
peptide biosynthetic process (GO:0043043)	1.9	0.0186
translational elongation (GO:0006414)	1.88	0.0227
translation (GO:0006412)	1.88	0.0225
amide biosynthetic process (GO:0006412)	1.86	0.0132
peptide metabolic process (GO:0006518)	1.77	0.0216
nervous system development (GO:0007399)	1.76	0.00245
organonitrogen compound biosynthetic process (GO:1901566)	1.66	0.00135
cell development (GO:0048468)	1.63	0.0378
cellular amide metabolic process (GO:0043603)	1.62	0.0354
multicellular organism development (GO:0007275)	1.55	0.00216
system development (GO:0048731)	1.53	0.0056
cell differentiation (GO:0030154)	1.51	0.00709
developmental process (GO:0032502)	1.51	0.0003
anatomical structure development (GO:0048856)	1.5	0.00118

D



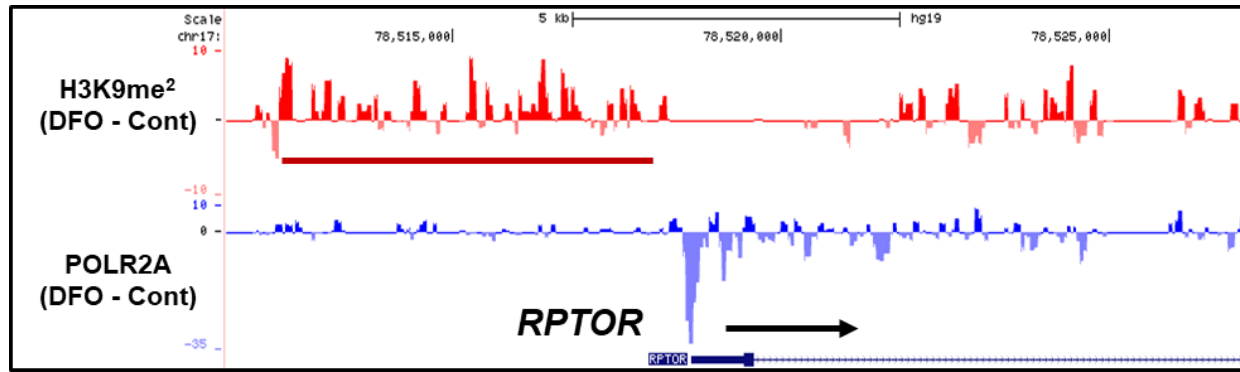
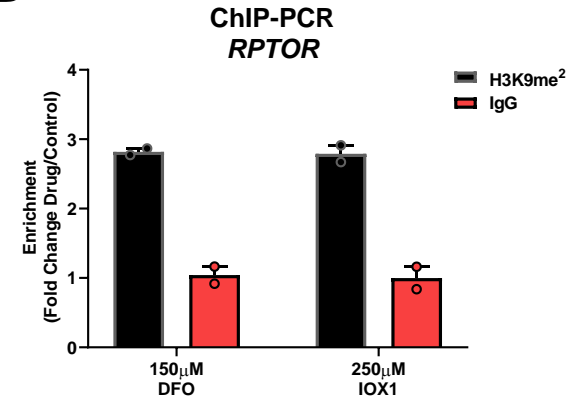
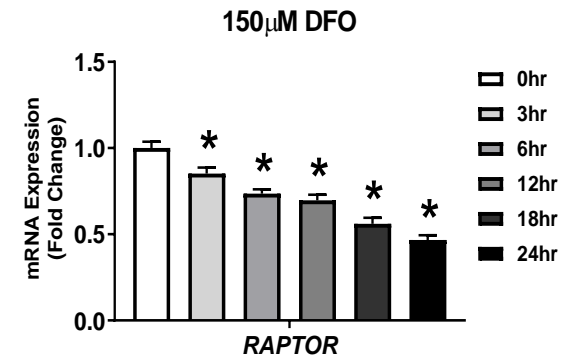
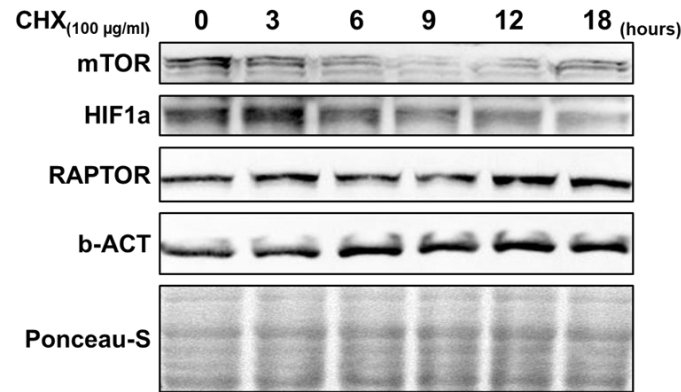
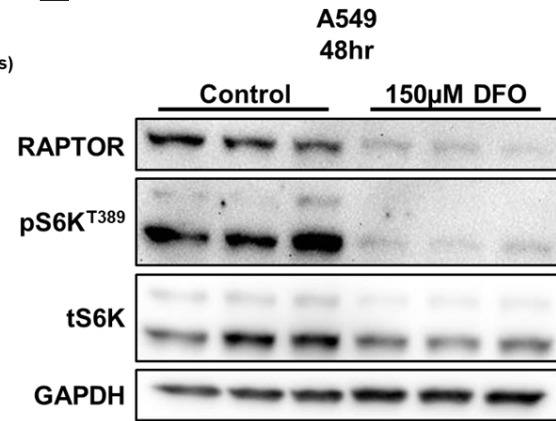
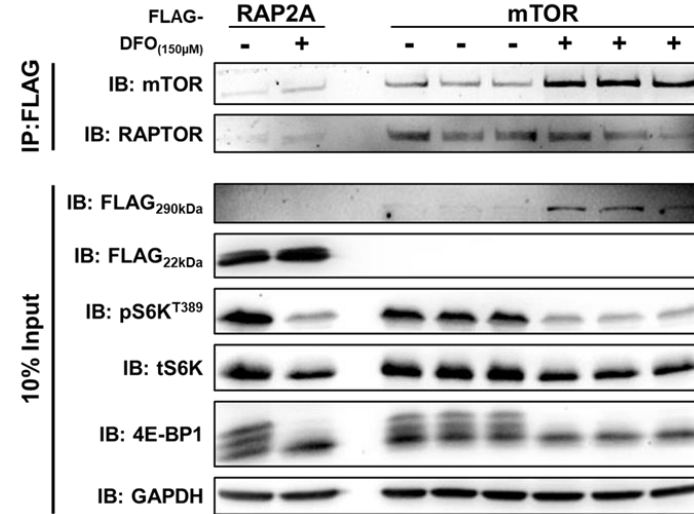
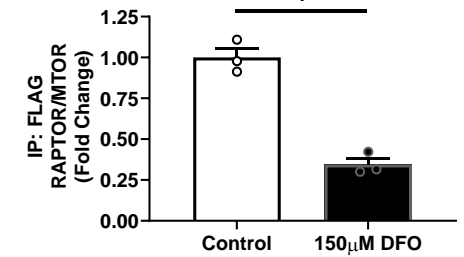
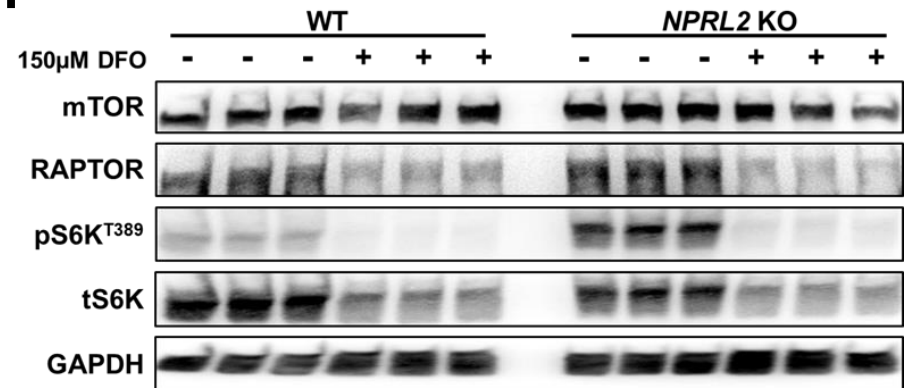
Encode Histone Color Code

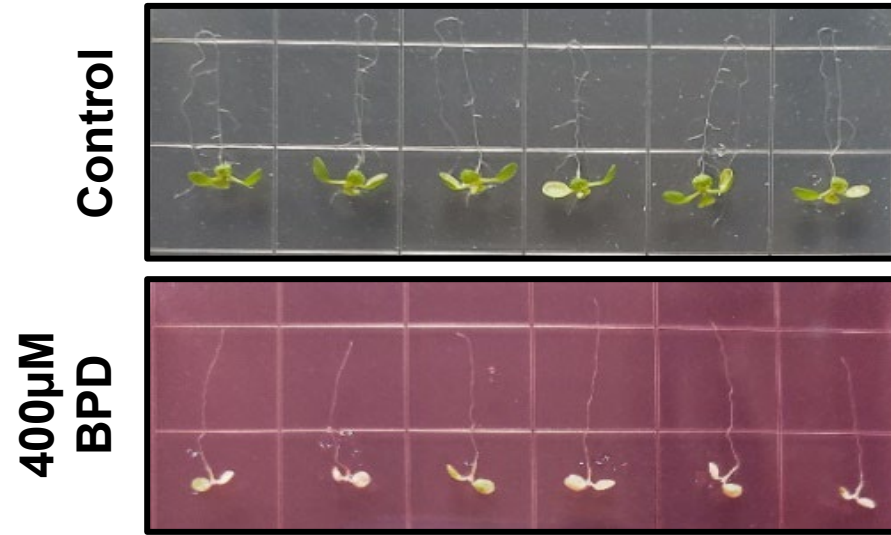
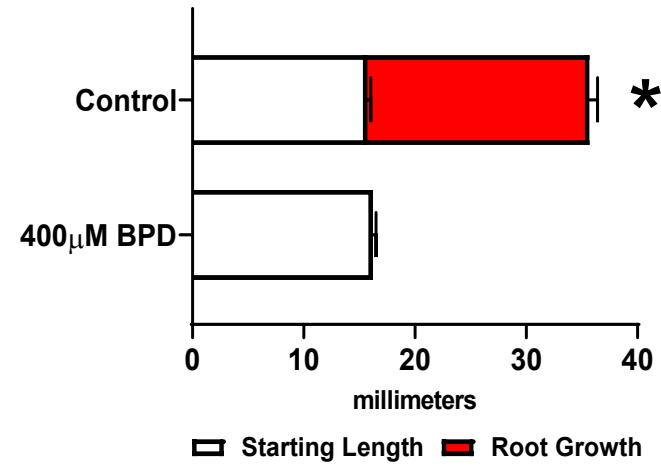
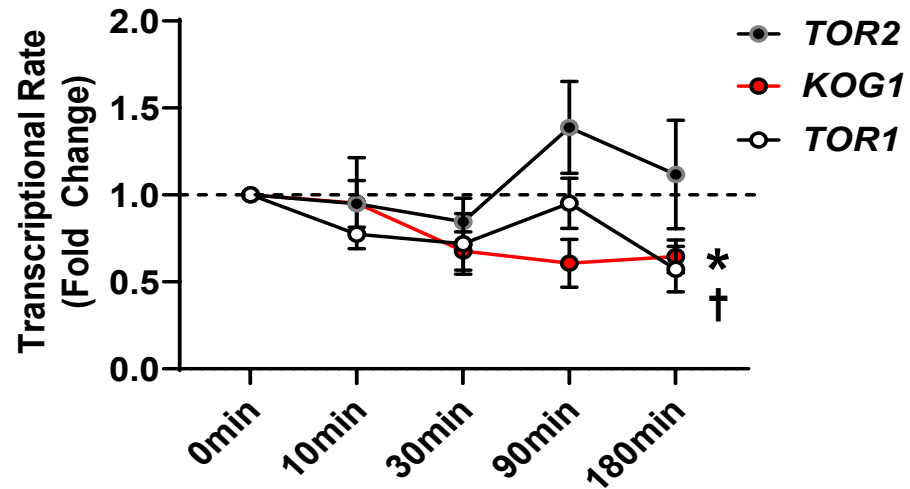
Green: Transcription
 Red: Active Promoter
 Yellow/Orange: Enhancer
 Purple: Poised Promoter
 Grey: Heterochromatin

Genehancer Color Code

Red: Promoter
 Grey: Enhancer Element

Figure S13

A**B****C****D****E****F****G****H****Figure S14**

A***Arabidopsis thaliana*****B****Root Growth****C*****Saccharomyces cerevisiae***
Strain: BY4741

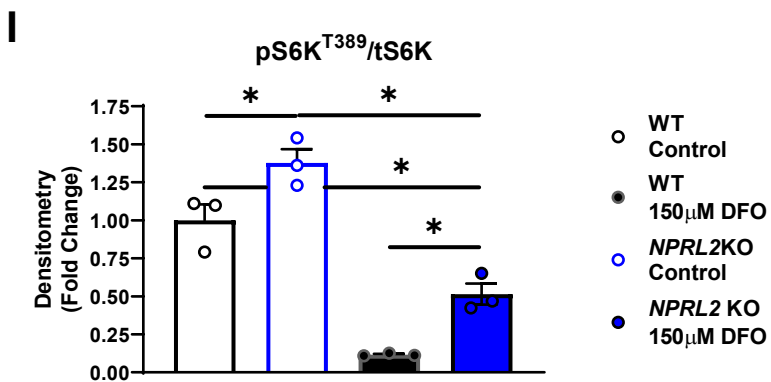
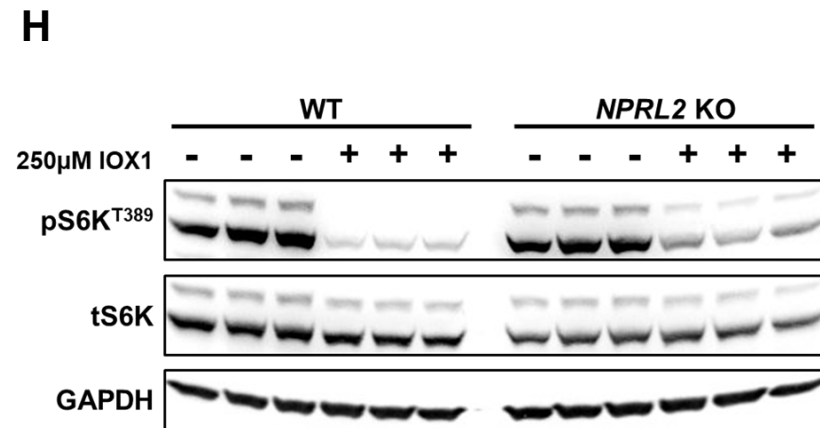
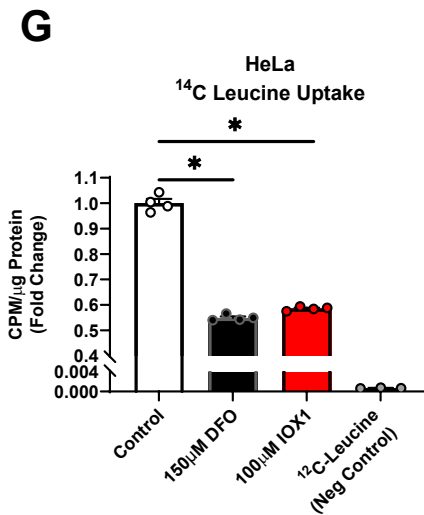
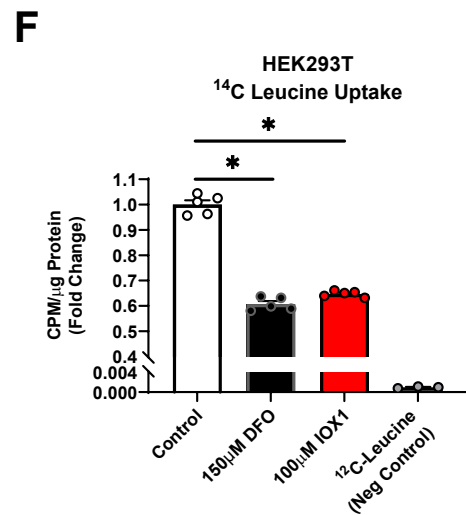
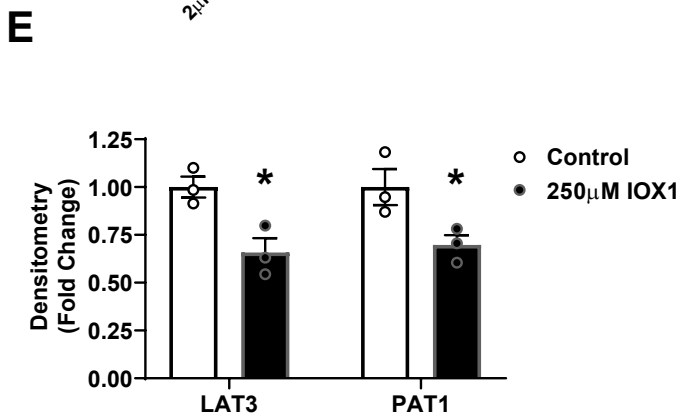
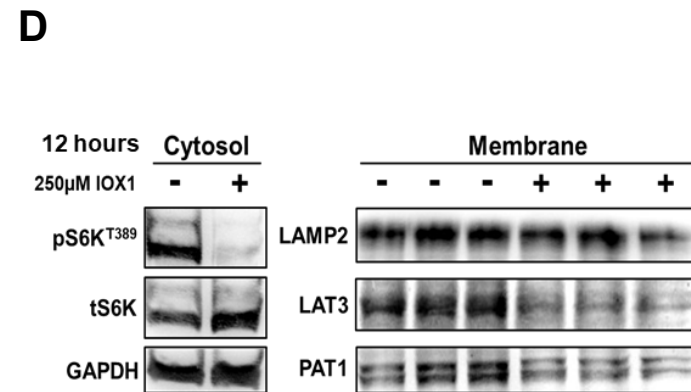
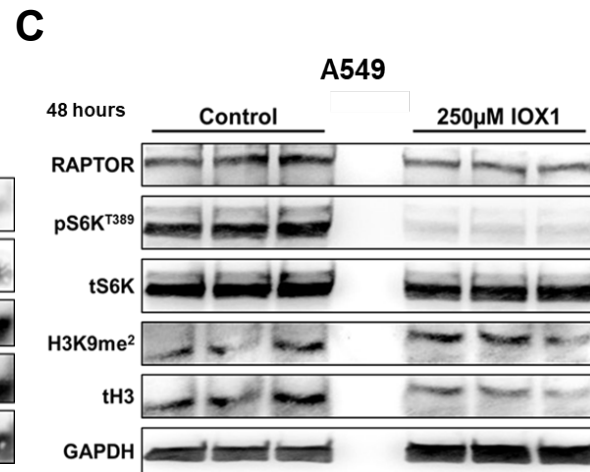
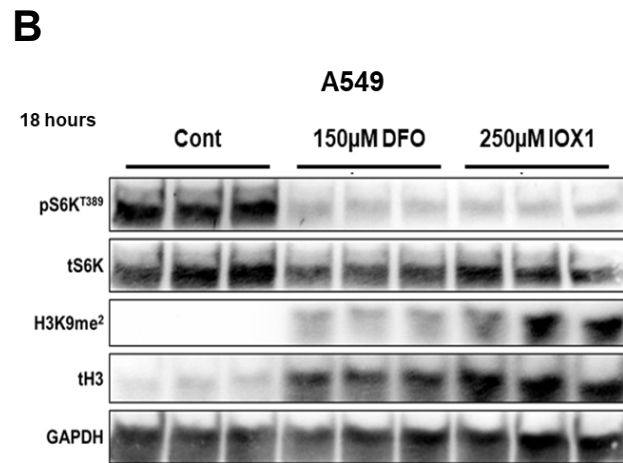
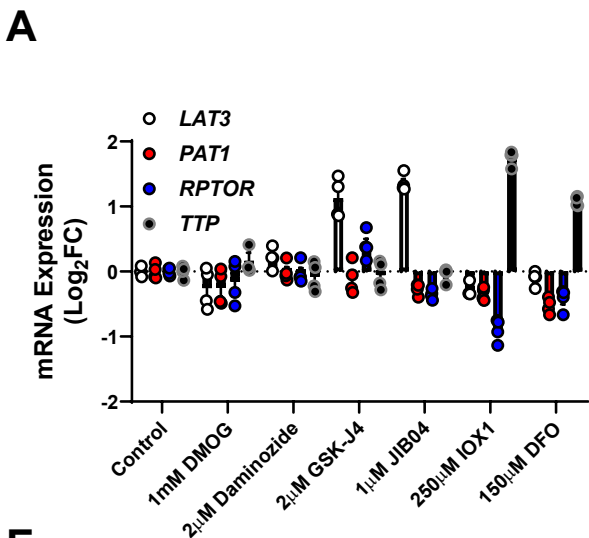


Figure S16

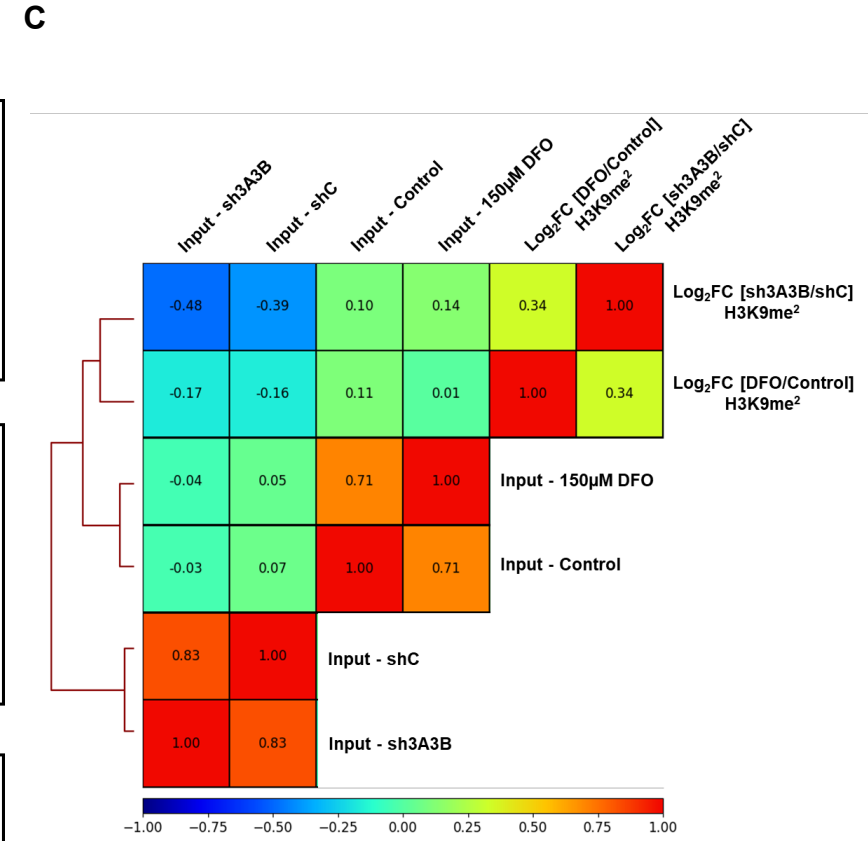
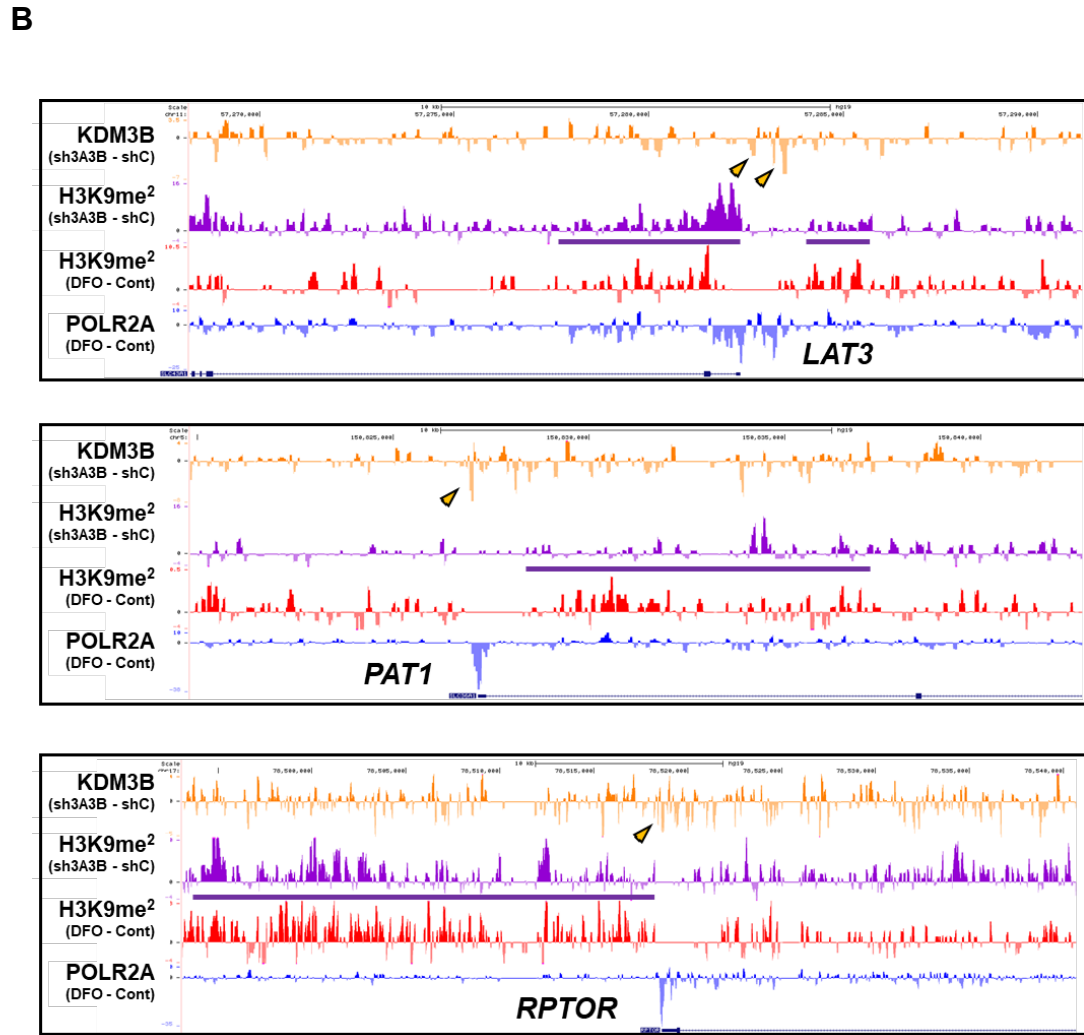
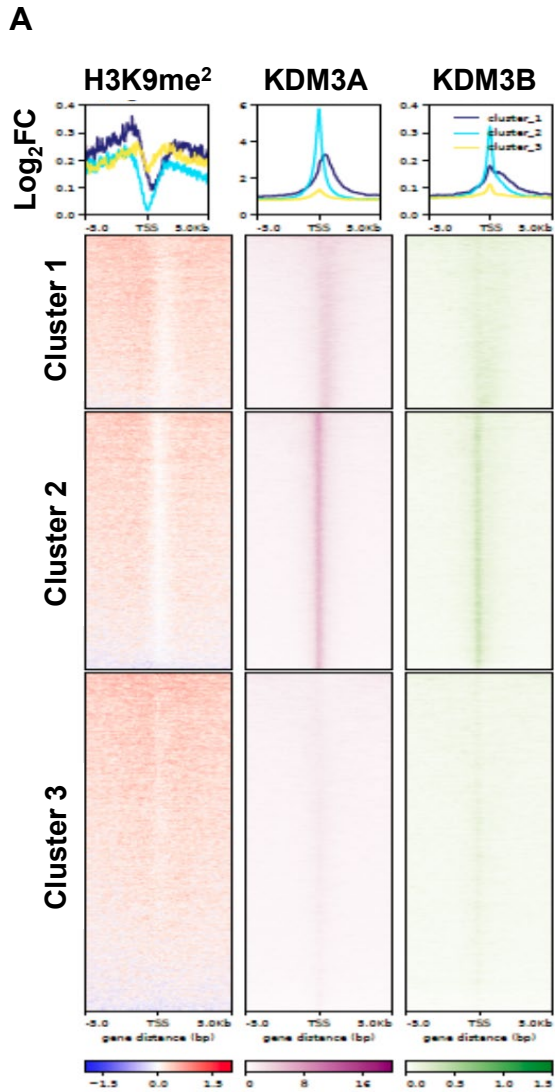


Figure S17

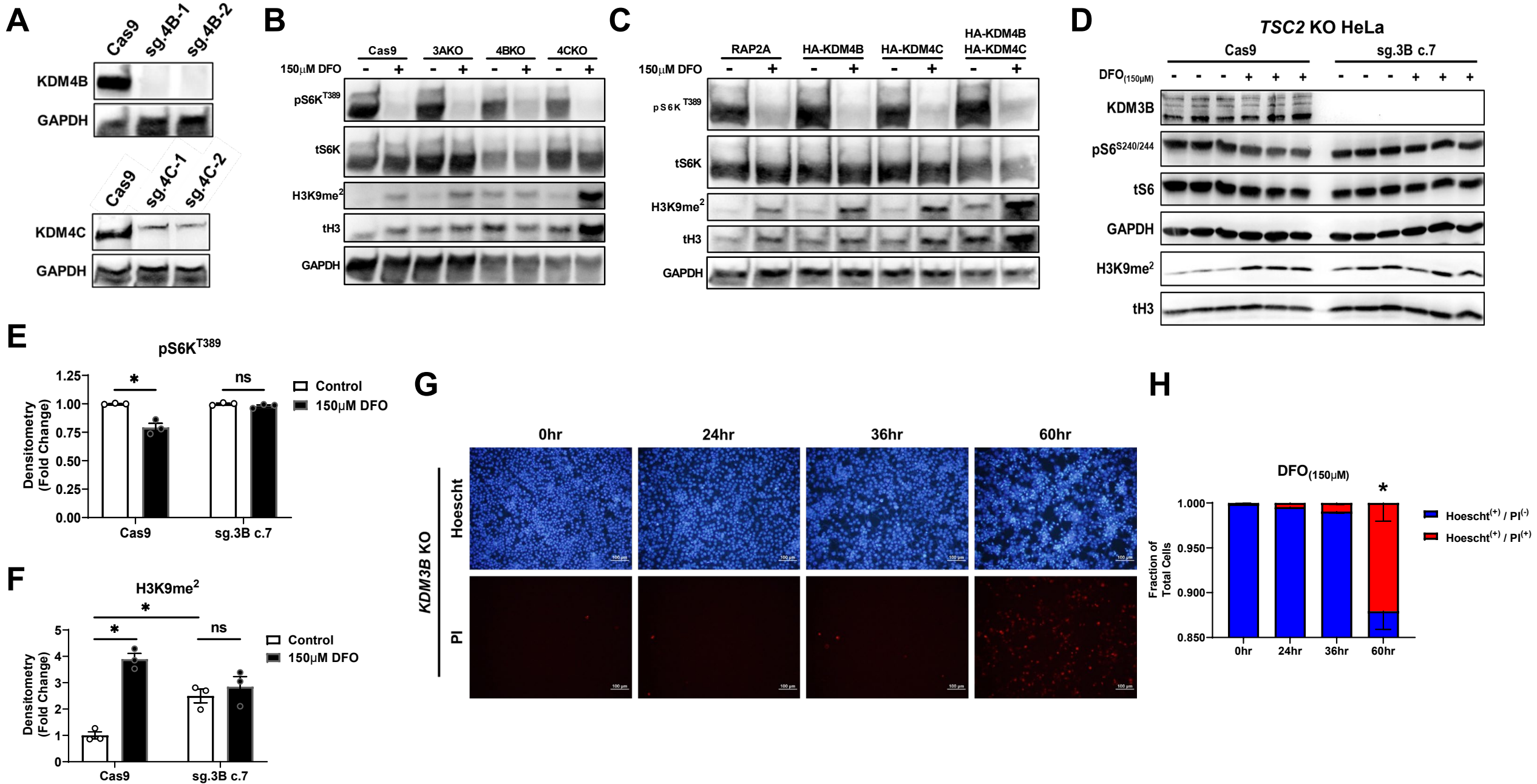


Figure S18

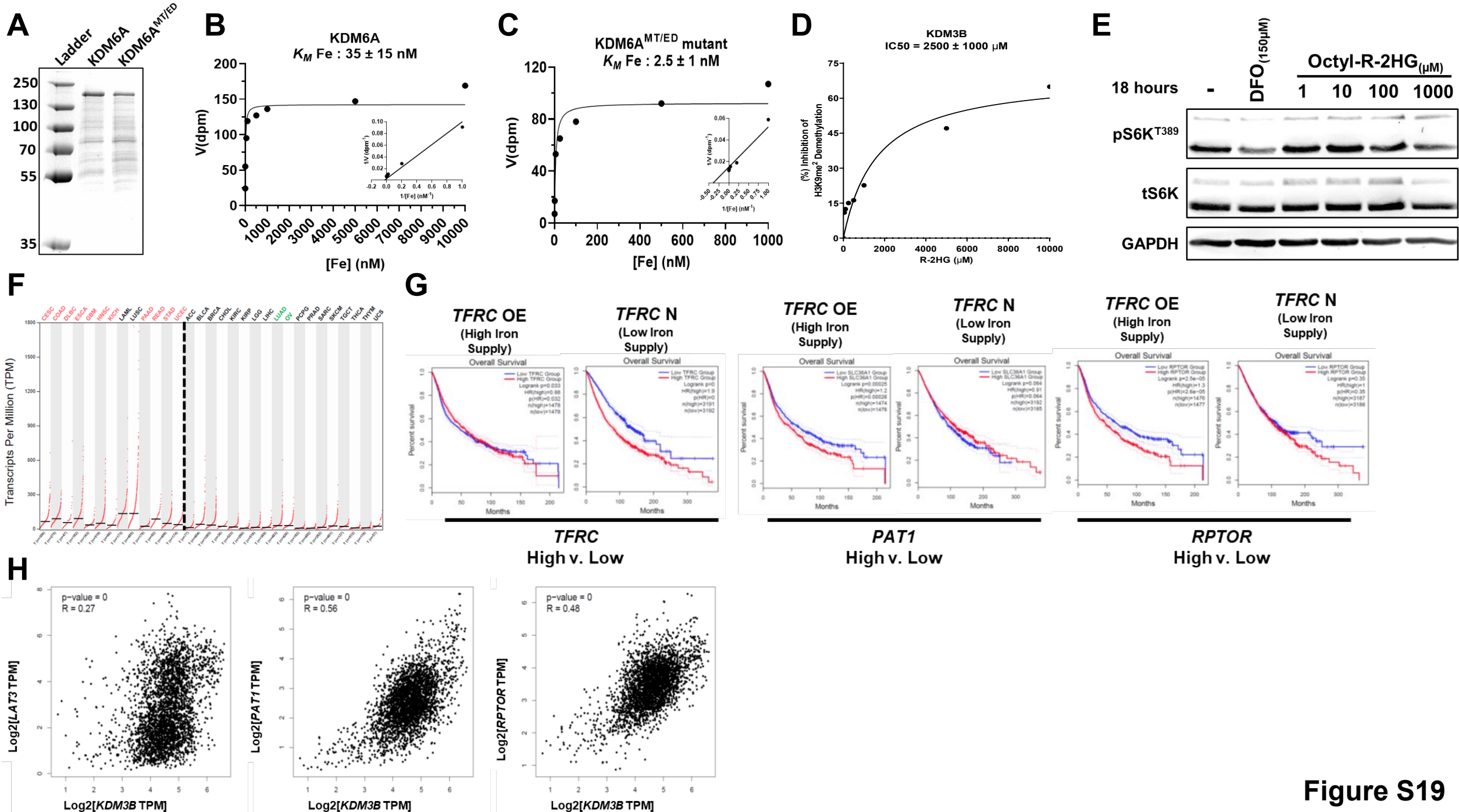
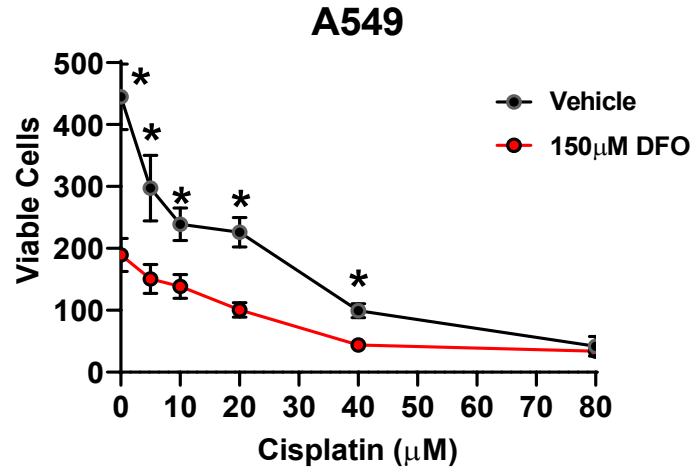
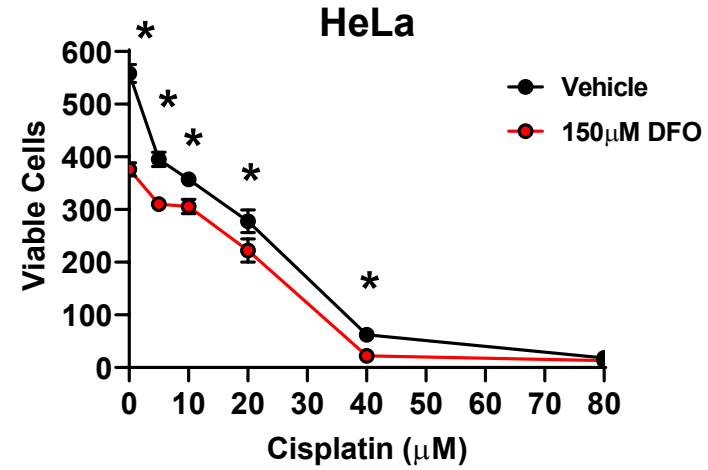
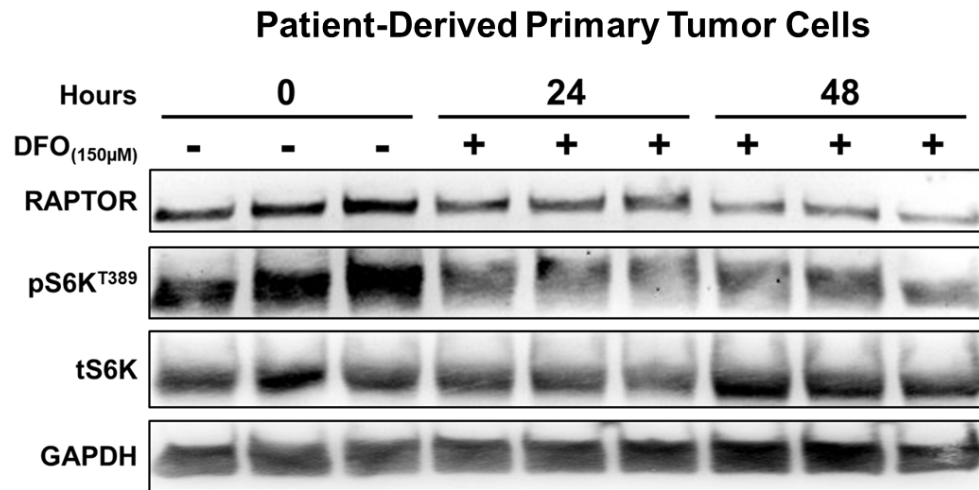
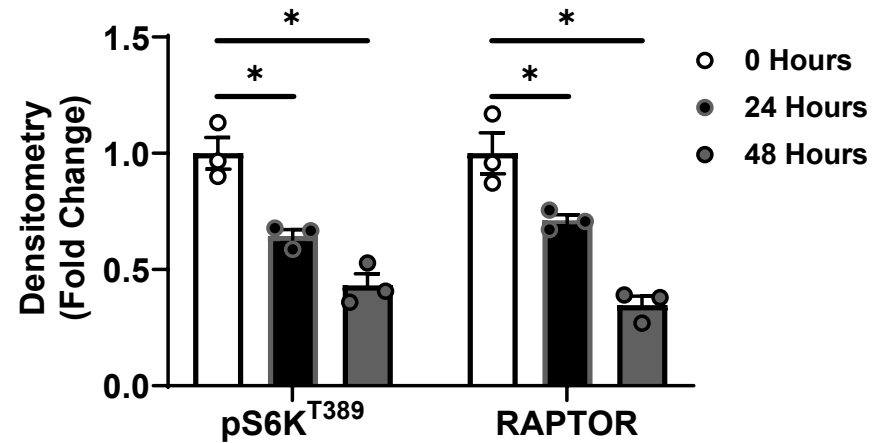


Figure S19

A**B****C****D****Figure S20**